USGS
science for a changing world

Evaluation of the Analytical Methods Used to Determine the Elemental Concentrations Found in the Stream Geochemical Dataset Compiled for Alaska

Open-File Report 2020–1038

Evaluation of the Analytical Methods Used to Determine the Elemental Concentrations Found in the Stream Geochemical Dataset Compiled for Alaska

By Bronwen Wang, Karl J. Ellefsen, Matthew Granitto, Karen D. Kelley, Susan M. Karl, George N.D. Case, Doug C. Kreiner, and Courtney L. Amundson

U.S. Department of the Interior
U.S. Geological Survey

For more information on the USGS—the Federal source for science about the Earth,
its natural and living resources, natural hazards, and the environment—visit
https://www.usgs.gov/ or call 1–888–ASK–USGS (1–888–275–8747).

For an overview of USGS information products, including maps, imagery, and publications,
visit https://store.usgs.gov/.

Contents

Figures

Tables

Conversion Factors

U.S. customary units to International System of Units

Multiply	By	To obtain
Mass		
ounce, avoirdupois (oz)	28.35	gram (g)
pound, avoirdupos (lb)	0.4536	kilogram (kg)

International System of Units to U.S. customary units

Multiply	By	To obtain
Length		
millimeter (mm)	0.03937	inch (in.)
centimeter (cm)	0.3937	inch (in.)
Volume		
milliliter (mL)	0.03381402	ounce, fluid (fl. oz)
Mass		
gram (g)		ounce, avoirdupois (oz)

Datum

Horizontal coordinate information is referenced to the North American Datum of 1983 (NAD 83).

List of Chemical Element Symbols

Element symbol	Element name
Ag	Silver
Al	Aluminum
As	Arsenic
Au	Gold
B	Boron
Ba	Barium
Be	Beryllium
Bi	Bismuth
Ca	Calcium
Cd	Cadmium
Ce	Cerium
Cl	Chloride
Co	Cobalt
Cr	Chromium
Cs	Cesium
Cu	Copper
Dy	Dysprosium
Er	Erbium
Eu	Europium
Fe	Iron
Ga	Gallium
Gd	Gadolinium
Ge	Germanium

List of Chemical Element Symbols—Continued

Element symbol	Element name
Hf	Hafnium
Hg	Mercury
Ho	Holmium
In	Indium
Ir	Iridium
K	Potassium
La	Lanthanum
Li	Lithium
Lu	Lutetium
Mg	Magnesium
Mn	Manganese
Mo	Molybdenum
Na	Sodium
Nb	Niobium
Nd	Neodymium
Ni	Nickel
Os	Osium
P	Phosphorus
Pb	Lead
Pd	Palladium
Pm	Promethium
Pr	Praseodymium
Pt	Platinum
Rb	Rubidium
Re	Rhenium
Rh	Rhodium
Ru	Ruthenium
Sb	Antimony
Sc	Scandium
Se	Selenium
Si	Silicon
Sm	Samarium
Sn	Tin
Sr	Strontium
Ta	Tantalum
Tb	Terbium
Te	Tellurium
Th	Thorium
Ti	Titanium
Tl	Thallium

List of Chemical Element Symbols—Continued

Element symbol	Element name
Tm	Thulium
U	Uranium
V	Vanadium
W	Tungsten
Y	Yttrium
Yb	Ytterbium
Zn	Zinc
Zr	Zirconium

Abbreviations

AA	atomic absorption
AGBD	Alaska Geochemical Database
AGDB2	Alaska Geochemical Database Version 2
AGDB3	Alaska Geochemical Database Version 3
AR	aqua regia
DC	direct-current
HCl	chemical formula for hydrochloric acid
$HClO_4$	chemical formula for perchloric acid
HF	chemical formula for hydrofluoric acid
HNO_3	chemical formula for nitric acid
ICP-AES	inductively coupled plasma-atomic emission spectrometry
ICP-MS	inductively coupled plasma-mass spectrometry
Kα	K-alpha emission lines in x-ray spectroscopy
NURE	National Uranium Resource Evaluation
ppm	parts per million
REE	rare earth elements consist of the lanthanide series of chemical elements; La, Ce, Pr, Nd, Pm, Sm, Eu, Gd, Tb, Dy, Ho, Er, Tm, Yb
USGS	U.S. Geological Survey

Method Abbreviations

Analytical method names and descriptions of the analytical techniques in Alaska Geochemical Database Version 2.0 (AGDB2) (Granitto and others, 2013).

Note: "Decomposition" used in the text is synonymous with the use of the term "digest" in this table.

Analytical method	Description
AA_CV	Mercury by cold vapor-atomic absorption spectrometry after multi-acid digestion and solution.
AA_F_AZ_Fuse_P	Silver, arsenic, bismuth, cadmium, copper, lead, antimony and zinc by flame atomic absorption spectrometry after partial digestion by K2S2O7 fusion, HCl-KI, ascorbic acid, and selective organic extraction with Aliquat 336-MIBK.
AA_F_AZ_H2O2_P	Silver, arsenic, bismuth, cadmium, copper, lead, antimony and zinc by flame atomic absorption spectrometry after partial digestion with HCl-H2O2-KI, ascorbic acid and selective organic extraction with Aliquat 336-MIBK.
AA_F_AZ_HCl_P	Silver, arsenic, bismuth, cadmium, copper, lead, antimony and zinc by flame atomic absorption spectrometry after partial digestion with HCl-KI, and selective organic extraction with Aliquat 336-MIBK.
AA_F_CX_P	Calcium, magnesium, sodium, potassium and cation exchange capability in soil by flame atomic absorption spectrometry after solution extraction and cation exchange.
AA_F_DTPA_P	Cadmium, cobalt, copper, iron, manganese, nickel, lead and zinc by flame atomic absorption spectrometry after DTPA extraction and cation exchange.
AA_F_Fuse	Major and minor elements by flame atomic absorption spectrometry after fusion digestion.
AA_F_Fuse_P	Molybdenum and antimony by flame atomic absorption spectrometry after K2S2O7 fusion partial acid digestion, and selective organic extraction with Aliquat 336-MIBK.
AA_F_H2O_P	Calcium, magnesium, manganese and arsenic in saturation paste of soil by flame atomic absorption spectrometry after solution extraction.
AA_F_HBr	Silver, gold and tellurium by flame atomic absorption spectrometry after HBr-Br2 digestion and selective organic extraction with Aliquat 336-MIBK.
AA_F_HCl_OE_P	Antimony by flame atomic absorption spectrometry after partial digestion with HCl and selective organic extraction with Aliquat 336-MIBK.
AA_F_HCl_P	Copper and manganese by flame atomic absorption spectrometry after partial digestion with HCl.
AA_F_HF	Major and minor elements by flame atomic absorption spectrometry after multi-acid digestion with HF.
AA_F_HNO3_P	Silver, cadmium, copper, lead and zinc by flame atomic absorption spectrometry after partial digestion with hot HNO3.
AA_FE	Sodium and potassium by flame emission spectrometry (flame photometry) after HF-HClO4 dissolution or LiBO2 fusion.

Analytical method	Description
AA_GF_HBr	Gold and tellurium by graphite furnace atomic absorption spectrometry after HBr-Br2 digestion and selective organic extraction with Aliquot 336-MIBK.
AA_GF_HF	Arsenic, gold, bismuth and tellurium by graphite furnace atomic absorption spectrometry after multi-acid digestion with HF and selective organic extraction with Aliquat 336-MIBK.
AA_GF_ST	Thallium by graphite furnace atomic absorption spectrometry after Na2O2 sinter, HCl-HNO3 dissolution, and selective organic extraction with DIBK.
AA_HG_Acid	Selenium by flow injection or continuous flow-hydride generation-atomic absorption spectrometry after digestion with HNO3-HCl-H2SO4-KMnO4.
AA_HG_HF	Arsenic, antimony, selenium and tellurium by flow injection or continuous flow-hydride generation-atomic absorption spectrometry after multi-acid digestion with HF.
AA_HG_ST	Arsenic and antimony by flow injection or continuous flow-hydride generation-atomic absorption spectrometry after Na2O2 sinter digestion.
AA_TR_W	Mercury by thermal release and atomic absorption spectrometry after heating (Vaughn-McCarthy method) and use of a willemite screen.
AES_Acid_P	Major and minor elements by inductively coupled plasma-atomic emission spectrometry after unknown partial acid digestion.
AES_AR_P	Major and minor elements by inductively coupled plasma-atomic emission spectrometry after partial digestion with aqua regia.
AES_AZ_P	Silver, arsenic, gold, bismuth, cadmium, copper, molybdenum, lead, antimony and zinc by inductively coupled plasma-atomic emission spectrometry after partial digestion with HCl-H2O2.
AES_Fuse	Major and minor elements by inductively coupled plasma-atomic emission spectrometry after fusion digestion.
AES_HF	Major and minor elements by inductively coupled plasma-atomic emission spectrometry after digestion with HF-HCl-HNO3-HClO4.
AES_HF_REE	Rare earth elements by ion exchange and inductively coupled plasma-atomic emission quantitative spectrometry after HF-HCl-HNO3-HClO4 digestion.
AES_IE	Molybdenum, niobium and tungsten by inductively coupled plasma-atomic emission quantitative spectrometry after HF-HCl-HNO3-HClO4 digestion and ion exchange separation.
AES_ST	Major and minor elements by inductively coupled plasma-atomic emission spectrometry after sinter digestion.
AFS_CV	Mercury in aqueous media by flow injection-cold vapor-atomic fluorescence spectrometry.
CB_CHN	Carbon, hydrogen and nitrogen by gas chromatography/thermal conductivity (CHN elemental) analyzer after combustion.
CB_IRC	Carbon and sulfur by infrared detection after combustion.
CB_TC	Total carbon and organic carbon by thermal conductivity detection after combustion.

Analytical method	Description
CB_TT	Sulfur by iodometric titration after combustion.
CM_Acid	Bromine by colorimetry after acid digestion.
CM_Acid_P	Arsenic by modified Gutzeit apparatus confined-spot method colorimetry after partial digestion in KOH-HCl and chemical separation.
CM_CX_P	Heavy metal elements by colorimetry after partial extraction in aqueous ammonium citrate solution.
CM_Fuse	Major and minor elements by colorimetric spectrophotometry after fusion digestion.
CM_Fuse_P	Molybdenum and antimony by colorimetry after partial digestion by K2S2O7 fusion (Mo) or NaHSO4 fusion-HCl digestion (Sb, rhodamine B).
CM_H2O_P	Sulfate in saturation paste of soil by colorimetric titration after solution extraction.
CM_HF	Major and minor elements by colorimetric spectrophotometry after multi-acid digestion with HF.
CM_HFS	Fluorine by colorimetric spectrophotometry after H2SiF6 digestion and chemical separation.
CM_HNO3_P	Copper, lead and zinc by colorimetry after partial digestion with HNO3.
CM_PC_P	Uranium by paper chromatography after partial digestion with HNO3.
CM_ST	Chlorine by colorimetric spectrophotometry after Na2CO3 and ZnO sinter digestion.
CM_ST_P	Tungsten by colorimetry after partial digestion with carbonate sinter.
CP	Organic carbon, carbonate carbon and totals by computation.
DN	Uranium and thorium by delayed neutron activation counting.
EDX	Minor elements by energy- dispersive x-ray fluorescence spectrometry.
ES_H2O_P	Boron by semiquantitative direct-current arc emission spectrography after solution extraction.
ES_Q	Major and minor elements by quantitative direct-current arc emission spectrography.
ES_SQ	Major and minor elements by semiquantitative direct-current arc emission spectrography.
FA_AA	Gold, silver and platinum group elements by graphite furnace atomic absorption spectrometry after PbO fire assay chemical separation.
FA_DC	Gold by direct current plasma-atomic emission spectroscopy or atomic absorption spectrophotometry after PbO fire assay chemical separation.

Analytical method	Description
FA_ES	Gold and platinum group elements by direct-current arc quantitative emission spectrography after PbO fire assay chemical separation.
FA_MS	Platinum group elements by inductively coupled plasma-mass spectrometry after NiS fire assay chemical separation.
FL_HF	Beryllium, tin and uranium by fluorometry after multi-acid digestion with HF.
FL_HNO3	Selenium by fluorometry after digestion with HNO3-H3PO4.
GRC	Uranium by gamma counting.
GV	Density, moisture and weight by gravimetry; ash or loss on ignition by weight loss after heating at 900° C.
GV_Acid	Major and minor elements by gravimetry after acid digestion.
GV_CR	Major and minor elements by gravimetry for Classical Rock Analysis after unknown digestion method.
GV_Flux	Moisture, bound water and total water by heating and weight loss with flux.
GV_Fuse	Major and minor elements by gravimetry after fusion digestion.
IC	Chlorine, fluorine, nitrate, sulfate and phosphate by ion chromatography.
INST	pH by standard method combination pH electrode.
INST_P	Specific conductance by standard method conductivity electrode and pH by standard method combination pH electrode after partial digestion.
ISE_Fuse	Chlorine, fluorine and iodine by ion specific electrode after fusion digestion.
ISE_H2O	Chlorine by ion specific electrode after solution extraction.
ISE_HF	Chlorine by ion specific electrode after multi-acid digestion with HF.
MS_AR_P	Major and minor elements by inductively coupled plasma-mass spectrometry after partial digestion with aqua regia.
MS_HF	Major and minor elements by inductively coupled plasma-mass spectrometry after HF-HCl-HNO3-HClO4 digestion.
MS_ST	Major and minor elements by inductively coupled plasma-mass spectrometry after Na2O2 sinter digestion.
MS_ST_REE	Rare earth elements by inductively coupled plasma-mass spectrometry after Na2O2 sinter digestion.
NA	Major and minor elements by long or short count instrumental neutron activation analysis.

Analytical method	Description
pH	pH by standard method combination pH electrode.
TB_AR	Acid-soluble sulfate, sulfur and sulfide by turbidimetry after aqua regia digestion.
TT_Flux	Total water by Karl Fischer coulometric titration with flux after combustion.
TT_Fuse	Fe2O3 by titration after fusion, decomposition and precipitation.
TT_HCl	Carbonate carbon and carbon dioxide (acid soluble carbon) by coulometric titration after HClO4 digestion and extraction.
TT_HF	Ferrous oxide by colorimetric or potentiometric titration after HF-H2SO4 digestion.
VOL	Carbon dioxide or carbonate carbon by evolution after acid decomposition; aka "gasometric" or "manometric".
WDX_Fuse	Major and minor elements by wavelength dispersive x-ray fluorescence spectrometry after LiBO2 fusion digestion.
WDX_Raw	Chlorine, iodine and bromine by wavelength dispersive x-ray fluorescence spectrometry on raw sample.

Evaluation of the Analytical Methods Used to Determine the Elemental Concentrations Found in the Stream Geochemical Dataset Compiled for Alaska

By Bronwen Wang, Karl J. Ellefsen, Matthew Granitto, Karen D. Kelley, Susan M. Karl, George N.D. Case, Doug C. Kreiner, and Courtney L. Amundson

Abstract

A recent U.S. Geological Survey data compilation of stream-sediment geochemistry for Alaska contains decades of analyses collected under numerous Federal and State programs. The compiled data were determined by various analytical methods. Some samples were reanalyzed by a different analytical method than the original, resulting in some elements having concentrations reported by multiple analytical methods. Consideration of the analytical methods used to determine the elemental concentrations is an important step in a mineral prospectivity analysis. We used the compiled data to compare concentrations of barium (Ba), cobalt (Co), copper (Cu), chromium (Cr), nickel (Ni), lead (Pb), and zinc (Zn) determined by different analytical methods to show how simple data comparisons can identify bias and provide a general sense of the comparability of different analytical methods. The elements were selected because they have a range of geochemical properties that may affect the performance of different analytical procedures.

Generally, agreement between Ba, Co, Cu, Cr, Ni, Pb, and Zn concentrations is good for most quantitative methods that use a total decomposition of the sample. However, Cr concentrations typically were lower for methods using quantitative-instrumental analysis following a multi-acid dissolution technique that included hydrofluoric acid compared to those using sinter decomposition. Additionally, low- to middle-range concentrations for Co, Cr, Cu, Ni, Pb, and Zn by instrumental neutron activation (NA) and energy-dispersive x-ray spectroscopy (EDX) analyzed by the National Uranium Resource Evaluation (NURE) program have high uncertainty. Concentrations determined by methods that use partial decomposition of the sample generally correspond well to concentrations determined by methods that use a total decomposition technique, except for Ba and Cr. For Ba and Cr, partial decomposition techniques yield lower concentrations than those determined by methods that use a total decomposition technique. Comparison of Ba, Co, Cr, Cu, Ni, Pb, and Zn concentrations determined by semiquantitative visual six-step direct-current arc emission spectrography (ES_SQ) to those determined by quantitative methods using either a total or partial decomposition technique consistently show scatter that exceeds the values expected based on the range represented by the semiquantitative concentration.

1

The data compilation includes a best-value determination that was selected based on the analytical method from the all concentration data for that sample. Ba, Cr, Co, and Zn concentrations determined by NA usually are selected as the best-value determination. However, the NURE-NA method was designed for high throughput and the uncertainty associated with low- and mid-range concentrations is greater than that of the multi-acid method used to reanalyze many samples. Selection of the multi-acid method over the NURE-NA method for Ba, Co, and Zn could be warranted. Additionally, concentrations determined by ES_SQ usually are selected as the best-value determination over all methods that use a partial decomposition of the sample. Substitution of concentrations determined by methods that use a partial decomposition for those of ES_SQ may be warranted for Co, Cu, Ni, Pb, and Zn. Regardless of the selection of the best-value determination, the dataset remains a mixed method dataset and the uncertainty due to differences in analytical methodology must be considered when using the dataset.

Introduction

A stream-sediment geochemical dataset for Alaska was compiled by the U.S. Geological Survey (USGS) as part of the Alaska Geochemical Database Version 3.0 (AGDB3) and was used in the Geochemical Atlas of Alaska (Lee and others, 2016) and the statewide mineral prospectivity evaluations (Karl and others, 2016). The dataset contains decades of geochemical analyses for samples collected under numerous Federal and State programs (Granitto and others, 2019). Different analytical methods were used reflecting the varying scientific objectives and time periods of the programs. The compiled dataset includes all geochemical data from the source databases, regardless of the analytical method and, for most elements, concentration data by different analytical methods are included in the compilation.

Geochemical datasets that include results from different analytical methods are challenging to work with, in part, because of varying sensitivities of different analytical methods. When differences are systematic, bias between methods occurs. For example, a chemical digestion may not fully decompose refractory minerals, resulting in artificially low concentrations for elements that remain in the insoluble residues compared with concentrations determined following a more comprehensive digestion. Simple visual comparisons between the concentrations determined by different methods for the same sample can help identify bias and provide a general sense of the comparability of different analytical methods.

Thousands of samples in the dataset have element concentrations determined by more than one method. These duplicate analyses primarily are from reanalysis of samples collected by the National Uranium Resource Evaluation (NURE) program and USGS programs under subsequent Federal and State projects (Granitto and others, 2019). The largest reanalysis efforts were part of the USGS National Geochemical Survey project (U.S. Geological Survey, 2008) that reanalyzed NURE samples and a collaborative project between the USGS and the Alaska Division of Geological and Geophysical Surveys (Werdon and others, 2014, 2015a–e), which reanalyzed samples mostly from the Seward Peninsula and the eastern Alaska Range previously collected by the NURE program and USGS projects (fig. 1). Other smaller reanalysis efforts resulted in more localized sample distributions. The paired concentration data provide an opportunity to compare the concentration of an element determined in the same field samples by two or more methods. Factors to consider include the mineralogical residence of the element of interest, sample decomposition techniques, analytical range of the methods, and lower detection limit criteria. For illustration purposes, we compare barium (Ba), chromium (Cr), cobalt (Co), copper (Cu), nickel (Ni), lead (Pb), and zinc (Zn) concentrations determined by different

analytical methods for the same sample. These elements were selected because they commonly were analyzed and, consequently, (1) have numerous samples analyzed by more than one method, (2) have a range of geochemical characteristics, and (3) were used in recent mineral prospectivity analysis.
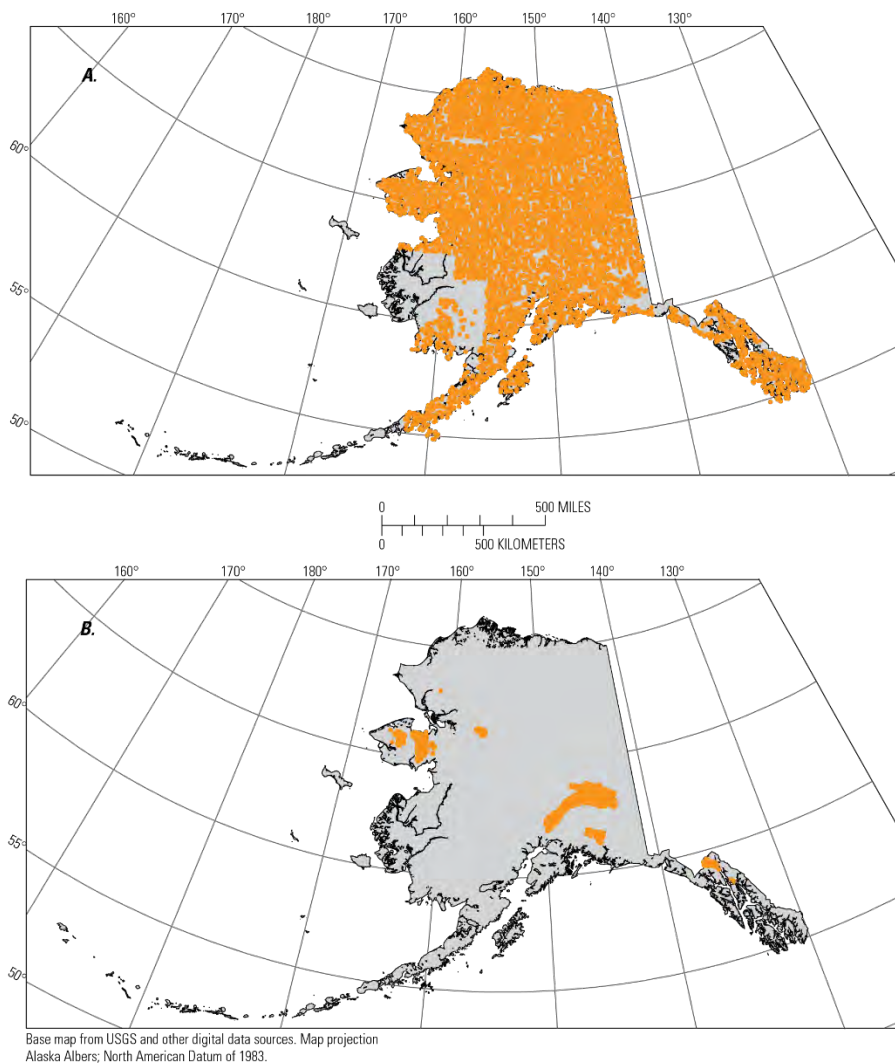
Figure 1. Maps showing spatial extent (shaded areas) of Alaskan samples reanalyzed by (*A*) the U.S. Geological Survey National Geochemical Survey project (U.S. Geological Survey, 2008), and (*B*) the Alaska Division of Geological and Geophysical Surveys (Werdon and others, 2014, 2015a–e).

Analytical Methods Common in the Paired Data

Semiquantitative visual six-step direct-current arc emission spectrography (ES_SQ) commonly was used in the USGS programs from the 1960s through the early 1990s. Samples analyzed by ES_SQ were frequent targets for reanalysis, as are the NURE program samples. The NURE program used instrumental neutron activation analysis (NA), delayed neutron activation counting (DN), and energy dispersive x-ray fluorescence spectrometry (EDX) for samples collected in Alaska (Information Systems Programs Energy Resources Institute, 1985). Multi-element methods involving multi-acid or sinter decomposition of the sample commonly were

3

used when samples were reanalyzed. Because of their prevalence in the comparisons, the ES_SQ methods used by USGS programs and the NA and EDX methods for the NURE program are briefly summarized here along with a brief discussion of chemical decomposition; a more extensive description of the ES_SQ, NA, and EDX methods and decomposition techniques are given in appendix 1.

The direct-current arc emission spectrography was used by the USGS to determine the concentrations of 30 elements. The method most frequently used was a semiquantitative method that subdivided each order of magnitude of concentration into six intervals per decade, known as the visual six-step method (Grimes and Marranzino, 1968; Motooka and Grimes, 1976). The steps were the approximate geometric midpoints of the concentration interval (table 1).

Table 1. Reported values and intervals of the semiquantitative visual six-step direct-current arc spectrographic analysis method (ES_SQ), in Alaska.

[All table numbers are given in parts per million]

Reported value	Interval[1]	Reported value	Interval[2]	Reported value	Interval[2]	Reported value	Interval[2]
1.5	1.2–1.8	15	12–18	150	120–180	1,500	1,200–1,800
2	1.8–2.6	20	18–26	200	180–260	2,000	1,800–2,600
3	2.6–3.8	30	26–38	300	260–380	3,000	2,600–3,800
5	3.8–5.6	50	38–56	500	380–560	5,000	3,800–5,600
7	5.6–8.3	70	56–83	700	560–830	7,000	5,600–8,300
10	8.3–12	100	83–120	1,000	830–1,200	10,000	8,300–12,000

[1]The interval values taken from Motooka and Grimes, 1976.

[2]The intervals are the order of magnitude of the intervals given in Motooka and Grimes,1976.

The NURE program in Alaska used NA analysis to determine the concentrations of 31 elements. In the NA method, stable isotopes of an element are transformed into radioactive isotopes by exposure to neutron irradiation. The decay times and counting intervals used by the Los Alamos Scientific Laboratory, the laboratory that analyzed most of the Alaska samples for the NURE program, facilitated throughput at the expense of maximum sensitivity (Hansel and Martell, 1977; Minor and others, 1982). The detection limits reported for each element determined by NA are a function of the total composition and mass of the individual sample. Concentrations were considered less than the detection limit of the system when the statistical counting error of short-lived gamma activity exceeded 50 percent (Information Systems Programs Energy Resource Institute, 1985).

The NURE program in Alaska used EDX analysis to determine the concentration of nine elements including Cu, Ni, and Pb (appendix 1, table 1.1). Analysis was performed on loose powder preparations. The detection limits established for the EDX procedure were 3 times the standard deviation of 10 measurements of a blank (appendix 1,table 1.1); the precision, determined based on 10 measurements of sand spiked at 20 and 100 parts per million (ppm), was less than 30 percent for Pb, Cu, and Ni, respectively, at 20 ppm, and less than 10 percent for the 100 ppm spikes (Hansel and Martell, 1977). The high Nb detection limit results from molybdenum Compton interference (Hansel and Martell, 1977).

Chemical decomposition of geologic samples is not required prior to analysis by ES_SQ, NA, DN, or EDX, but most of the methods required chemical decomposition prior to instrumental analysis. For example, a method involving elemental analysis by inductively coupled plasma-mass spectrometry or atomic-emission spectrometry analysis following sample decomposition by a multi-acid mixture, which included hydrofluoric acid, was used in the reanalysis of the NURE samples by the USGS National Geochemical Survey project. Acid and flux decomposition techniques are common means of preparing samples for spectrometric instrumental analysis (Chao, 1984; and Chao and Sanzolone, 1992). Important characteristics for acid decomposition include the oxidizing power of an acid and its efficiency in breaking the silicon-to-oxygen bond in silicate minerals. Whether a flux is alkali or acid and oxidizing or reducing in a reaction are important considerations (appendix 1, tables 1.2 and 1.3; Chao and Sanzolone, 1992). Other considerations are the possible loss of elements due to formation of volatile compounds such as formation of volatile fluorides of As, B, Ti, Nb, Ta, Ge, Sb, and Si during dissolution with HF; the formation of insoluble compounds; the availably of high purity acids or fluxes; and, for fluxes, the flux composition relative to the elements of interest (Na and Li cannot be determined in a sample decomposed by fluxes containing Na and Li, respectively) (Chao and Sanzolone, 1992). Following chemical decomposition, various analytical instruments were used to determine the element concentrations.

The extent of sample decomposition varies depending on the chemical decomposition or dissolution technique used and the minerology of the sample. "Total" and "partial" are terms commonly used to describe decomposition techniques. Acid dissolution and flux decomposition can be considered total or partial decomposition techniques depending on the decomposition protocol (Chao, 1984; Chao and Sanzolone, 1992). "Total" and "partial" are inexact terms and the extent of decomposition will depend on the mineralogy of the sample. Nonetheless, these terms are a common means of characterizing chemical decomposition techniques (Chao and Sanzolone, 1992) and are used to classify methods in the Alaska Geochemical Database (AGBD) (Granitto and others, 2011, 2013, 2019). In the AGBD, total methods are those that used a total decomposition technique and partial methods are those that used a partial decomposition technique. Although ES_SQ, EDX, and NA do not require chemical decomposition, they are classified as total methods in the AGBD because the entire sample aliquot is vaporized or irradiated. Throughout this document, method abbreviation used in the Alaska Geochemical Database Version 2.0 (AGBD2) (Granitto and others, 2013) are used to identify methods (see section, "Method Abbreviations" for definitions). Abbreviations generally follow this format:

Analytical instrument abbreviation_decomposition technique abbreviation.
For example, MS_ST is the abbreviation for a method with elemental analysis by inductively coupled plasma-mass spectrometry (MS) and sample decomposition by a sinter technique (ST). The AGBD2 classification of a method as a partial or total method is used to group the methods for the paired analysis. These terms are inexact, and any decomposition technique can be total or partial depending on the mineralogy of the sample. Methods designated in the AGBD2 as having a partial decomposition technique have a "_P" suffix attached to the method abbreviation (for example, AA_F_HNO3_P, see section, "Method Abbreviations" for the method description).

Data and Data Handling

The "best-value" presentation of the combined dataset includes an element summary column that contains all concentration measurements and the associated analytical methods (Granitto and others, 2013, 2019). The summary column was used to identify samples with

concentrations of Ba, Cr, Co, Cu, Ni, Pb, and Zn determined by more than one analytical method. When the same method appeared twice in the summary column, indicating that the sample was run more than once by the method, the analytic values associated with the multiple analyses were averaged. Some samples determined by ES_SQ had concentration data that were recorded as values other than those of the six-step method. When this occurred, the data were placed at the value that corresponded to the appropriate six-interval value based on the ES_SQ intervals given in table 1. Tables 2, 3, and 4 (at back of report) list the methods used to analyze Ba, Cr, Co, Cu, Ni, Pb, and Zn concentrations and, for each method, the number of samples analyzed, the range of detected values, and the range of left-censored values (values reported as less than a value).

Samples with the same combinations of methods were identified, the number of samples with each method combination were counted (for example, 5,890 samples were analyzed for Ba by both the AES_HF and NA methods [see section, "Method Abbreviations" for method descriptions]; tables 5, 6, and 7 at back of report), and the spatial distributions of the paired analysis were plotted. Binary plots were constructed between all method pairs that had 50 or more determinations that were not left-censored (data reported as less than a value) in either method (that is, all determinations for both methods used in the plots had detectable concentrations; figs. 2–8, at back of report).

To aid in discussion, plots were augmented with the 1-to-1 line (black line) and the lines representing 1.5, 3.5, 7.5, and 15.5 times the element's background concentration (dashed pink lines). Bias between measurements was visually evaluated relative to the 1-to-1 line; data that consistently plot above or below the 1-to-1 line are positively or negatively biased, respectively. For plots with ES_SQ as one of the methods, small green boxes corresponding to the size of the interval associated with the reported ES_SQ concentration also were added (figs. 2*C*, 3*C*, 4*C*, 5*C*, 6*C*, 7*C*, and 8*C*, at back of report). The AGBD2 classification of methods as total or partial was used to group the paired analyses into total to total method pairs, total to partial method pairs, and semiquantitative to total method pairs, (semiquantitative to partial method pairs and partial to partial method comparisons were made but are not discussed in this report).

Comparisons of Elemental Concentrations

Data from sample reanalysis provide an opportunity to compare concentration data determined by different analytical methods. For Ba, Cr, Co, Cu, Ni, Pb, and Zn comparisons between two methods are shown in figures 2–8 (at back of report). The following discussion is organized by the categories of the methods (e.g. comparison between two total methods, between a total and a partial method, and ES_SQ and a total method).

Comparison of Total Methods

A list of total methods used to determine Ba, Cr, Co, Cu, Ni, Pb, and Zn concentrations available in the compiled dataset are given in table 2. The combinations of total methods are given in table 5 along with the number of samples and the number of pairs that have detected concentrations by both methods. Figures 2*A*, 3*A*, 4*A*, 5*A*, 6*A*, 7*A*, and 8*A* show the paired concentration data, the corresponding 1-to-1 line, and the spatial distribution of the samples with paired analysis. Only samples that had detected concentrations by both methods are shown. The spatial distribution is different for each comparison. Reanalysis of the NURE samples under the USGS National Geochemical Survey project resulted in a statewide distribution of samples with

concentration data for Ba, Co, Cr, and Zn by both NA and AES_HF and Cu, Ni, and Pb concentrations by both EDX and AES_HF (U.S. Geological Survey, 2008; figs. 2*A*, 3*A*, 4*A*, 5*A*, 6*A*, 7*A*, and 8*A*). Other efforts resulted in concentration data derived from other combinations of total methods, but fewer samples with more restricted sample distributions were analyzed (table 2; figs. 2*A*, 3*A*, 4*A*, 5*A*, 6*A*, 7*A*, and 8*A*).

EDX Compared to AES_HF, and NA Compared to AES_HF

Scatter is considerable around the 1-to-1 line in the low- to mid-range of the Cu, Ni, and Pb concentrations determined by both AES_HF and EDX, but agreement improves at higher concentrations (figs. 5*A*, 6*A*, and 7*A*). Ba, Co, Cr, Ni, and Zn analysis by NA and AES_HF are available for many reanalyzed samples (figs. 2*A*, 3*A*, 4*A*, 6*A*, and 8*A*). The scatter around the 1-to-1 concentration line is fairly symmetrical for Ba concentrations determined by NA and AES_HF. The scatter is symmetrical over the entire concentration range (about 55 to >10,000 ppm; fig. 2*A*) but it seems to diminish at concentrations greater than about 2,000 ppm. In contrast, scatter around the 1-to-1 line for Co and Zn concentrations of less than about 60 and 300 ppm, respectively, is slightly asymmetrical. The scatter between the Co and Zn concentrations determined by NA and AES_HF seems to diminish at higher concentrations (figs. 3*A* and 8*A*). For Cr concentrations determined by NA and AES_HF, the scatter is extremely asymmetrically distributed over the entire concentration range (about 4 to 800 ppm; fig. 4*A*). The Cr concentrations determined by NA typically are greater than those determined by AES_HF (that is, the samples tend to plot above the 1-to-1 line).

Cu, Ni, and Pb by EDX and AES_HF, and Ba, Co, Cr, and Zn by NA and AES_HF, all show increased scatter at lower concentrations (figs. 2*A*, 3*A*, 4*A*, 5*A*, 6*A*, 7*A*, and 8*A*). Increasing scatter at lower concentrations is expected because uncertainty, even if only a few parts per million, will produce a flaring of the scatter on log-log plots (Ludington and others, 2006). However, an additional consideration is the derivation of the lower detection limit. Geochemical concentration data less than some value are reported as less than that value (that is, the data are left-censored). Various terms—such as detection limit, limit of detection, limit of determination, limit of quantification, and reporting limits—have been used as the left-censoring threshold but lack of adherence to a single definition for the terms makes comparison across methods difficult unless the definition of the term is given (Potts, 1992; Taggart, 2002). Because of differences in the censoring threshold used by the NURE and the reanalysis programs, some of the scatter observed at lower concentrations could relate to the threshold used.

The detection limit for the EDX method used during the NURE program was defined as 3 times the standard deviation (σ) of 10 measurements of a blank sample. Signals at the 3σ level have high uncertainty and often are considered the threshold of quantitative analysis (Potts, 1992). The 3σ values for Cu, Ni, and Pb by the EDX method used during the NURE program are 10, 15, and 5 ppm, respectively (appendix 1, table 1.1; Information Systems Programs Energy Resources Institute, 1985). The Cu, Ni, and Pb concentrations determined for the NURE program were left-censored at or near the 3σ values (table 2). The precision of the NURE program's EDX method was determined on sand samples that were spiked with the elements of interest at either 20 or 100 ppm. At 100 ppm, the relative standard deviation was 10 percent or less, and at 20 ppm, it was 38 percent or less (Hansel and Martell, 1977). Whether the precision was determined by repeated measurement of the same loose powder preparation or if separate preparations were made is unclear. If the precision was determined on multiple measurements of the same preparation, it represents the instrumental precision and does not include loss of

precision due to sample preparation. The 3σ values for the AES_HF method based on 30 blank measurements are given in appendix 1, table 1.1, but they were not the values used as the left-censoring threshold because limits that are based solely on blanks do not account for matrix effects (Lichte and others, 1987; Potts, 1992; Briggs, 2002). Instead, reporting limits were defined for the AES_HF method used by the USGS and samples were censored at or near these limits (Briggs, 2002; appendix 1, tables 1 and 2). How the reporting limits for the AES_HF method were determined is not explicitly stated but they are higher than the 3σ values and incorporate matrix effect considerations (Briggs, 2002). The precision of the method determined on duplicate measurements of separate preparations of geologic reference samples was 10 percent or better at 10 times the reporting limits, and the precision of the analysis was about 0.5 relative standard deviation for analysis of the same sample solution (Lichte and others, 1987). The reporting limits for Cu, Ni, and Pb concentrations by the AES_HF method are 2, 3, and 4 ppm, respectively, and the uncertainty would be 10 percent or less at 20, 30, and 40 ppm, respectively; a comparable level of uncertainty is obtained at about 100 ppm for the NURE EDX method. Although some ambiguity surrounds the quality-control information of the methods, the above discussion suggests that the level of uncertainty in the EDX analysis is greater than that of AES_HF at lower ends of the concentration range because of the differences in how the data were left-censored.

Agreement is relatively good between Ba concentrations determined by NA and AES_HF, but scatter is considerable between the Cr, Co, and Zn concentrations. An early publication reported minimum detection limits for the NA method used at Los Alamos National Laboratory to analyze the NURE samples as 300, 20, 2, and 20 ppm for Ba, Cr, Co, and Zn, respectively (Nunes and Weaver, 1978). These limits later were characterized as "typical" lower detection limits for the NA analyses (Bolivar, 1987). "Average" detection limits determined based on a 4-g sample of "typical" sediment for the NA analyses also were reported (Minor and others, 1982). For Ba, Cr, Co, and Zn, the "average" detection limits are 150, 10, 1.7, and 11 ppm, respectively (the detection limit for Zn reported by Minor and others [1982] and that reported in Information Systems Programs Energy Resources Institute [1985] differ; the latter publication gives the detection limit of zinc as 100 ppm). Minor and others (1982), Information Systems Programs Energy Resources Institute (1985), and Bolivar (1987) all state that "the uncertainty in the trace element concentrations was usually less than 10 percent at concentration values one order of magnitude above the detection limit" and the context suggests that this statement refers to the "typical" or "average" detection limits. This implies that at around 1,500 or 3,000 ppm for Ba; 100 or 200 ppm for Cr; 17 or 20 ppm for Co; and 110, 200, or 1,000 ppm for Zn, the uncertainty "usually" is less than 10 percent. The NURE data, however, were not censored at the "average" or "typical" detection limits but were censored on a sample-by-sample basis at the concentration corresponding to the point at which the statistical counting error of short-lived gamma activity exceeded 50 percent (Information Systems Programs Energy Resources Institute, 1985); this results in numerous left-censoring thresholds for Ba, Cr, Co, and Zn concentrations in the compiled dataset (table 2; fig. 9). The most common left-censoring threshold values (the mode of the left-censored data) for NURE samples in the dataset are 100 ppm for Ba, 10 ppm for Cr, 0.1 ppm for Co, and 200 ppm for Zn for samples from Alaska (table 2), which, except for Cr, are less than both the "typical" and "average" detection limits and suggests that the uncertainty exceeds 10 percent for the concentration values reported as less than the "average" detection limits. Reporting limits for the AES_HF method are 1 ppm for Ba and 2 ppm for Cr, Co, and Zn. The precision at 10 times the reporting limit is better than 10 percent

8

(Briggs, 2002). For Ba, Co, and Zn concentrations determined by AES_HF and NA, the scatter seems to diminish at concentrations greater than about 2,000 ppm for Ba, 50 ppm for Co, and 300 ppm for Zn, which corresponds to the region where uncertainty in the NA analysis would decrease to about 10 percent. Although ambiguity surrounds the quality-control information of the methods, the above discussion suggests that the uncertainty may be greater for the NA analysis for Ba, Co, and Zn than that of AES_HF at lower ends of the concentration range.

Other Total to Total Method Comparisons

Other comparisons of total methods include fewer samples that are more spatially localized than those of the AES_HF comparisons with NA or EDX (table 5; figs. 2*A*, 3*A*, 4*A*, 5*A*, 6*A*, 7*A*, and 8*A*). Over 700 samples have paired concentrations of Ba, Cr, Cu, Ni, and Zn from analyses by both AES_HF and AES_ST. The difference between these methods is the technique used to decompose the sample prior to the analysis of the resulting solution by inductively coupled plasma-atomic emission spectrometry: AES_HF uses a four-acid decomposition consisting of hydrochloric (HCl), nitric (HNO_3), perchloric ($HClO_4$), and hydrofluoric (HF) acids; AES_ST uses a sinter decomposition, most commonly a sodium peroxide flux, followed by dissolution of the resulting cake in dilute acid, typically dilute HNO_3. More than 600 samples have paired concentrations from analysis by AES_HF and MS_Fuse for Ba and Cr. These methods differ in both the decomposition and instrumental technique (see section, "Method Abbreviations"). Several hundred samples have detectable Co and Pb by analysis using MS_ST and MS_HF, which are methods that differ in the decomposition technique, and MS_ST and AES_HF, which are methods that differ in both decomposition and instrumental technique.

Agreement is good between Ba, Co, Cu, and Zn concentrations regardless of whether a multi-acid, sinter, or fusion decomposition was used and irrespective of instrumental technique (figs. 2*A*, 3*A*, 4*A*, and 8*A*). The good agreement between Ba concentrations determined by the AES_HF and AES_ST or MS_Fuse methods suggests that the four-acid decomposition used in the AES-HF method did not cause appreciable precipitation of Ba as an insoluble fluoride in these samples (fig. 2*A*; appendix 1, table 1.2). Agreement is relatively good between Ni concentrations determined by AES_HF and AES_ST, but at concentrations less than about 30 ppm, asymmetrical scatter is observed, and the concentrations determined by the AES_ST method generally are higher than those of the AES_HF method (fig. 6*A*). This suggests that dissolution of Ni-bearing minerals depends on the digestion techniques used. Cr concentrations by ASE_ST also are higher than determined by the AES_HF method, as are Cr concentrations determined by mass spectroscopy following fusion decomposition (MS_Fuse) compared to those determined by AES_HF and an ultra-trace version of the method (AES_HF_UT) (fig. 4*A*). Poor dissolution of Cr contained in resistant minerals by the multi-acid decomposition or the complexation with insoluble fluorides may be responsible for the differences. A positive bias at low concentrations is observed for Pb concentrations determined by MS_ST relative to those determined by AES_HF but agreement is good between Pb concentrations determined by MS_HF and MS_ST (fig. 7*A*). Instrumentation differences and (or) the uncertainty associated with concentrations near the left-censoring threshold likely are causes but, except for the AES_HF method, documentation is inadequate to evaluate these possibilities.

Comparison of Total to Partial Methods

Partial decomposition methods target metals bound to secondary minerals and were used to enhance the contrast between geochemical anomalies and background concentrations (Chao, 1984; Church and others, 1987). Partial methods commonly are designed not to affect silicate minerals and may not decompose resistate minerals. The extent of sample dissolution, however, depends on the nature of the extractant and the mineralogy of the sample. The compiled dataset includes Ba, Cr, Co, Cu, Ni, Pb, and Zn concentrations determined by partial methods (table 3). The methods use various decomposition techniques prior to instrumental analysis, including the commonly used 1:3 volume ratio mixture of HNO_3 and HCL—acids known as aqua regia (AR).

Ba, Cr, and Co only were reported for partial methods that use an AR digestion technique (table 3). Ba and Cr concentrations determined by partial methods AES_AR_P and MS_AR_P are low compared to those by total methods (figs. 2*B* and 4*B*). Agreement is better between Co concentrations determined by total methods MS_HF and NA and partial methods AES_AR_P and MS_AR_P, but agreement is poor between Co concentrations determined by AES_HF and AES_AR_P (fig. 3*B*). Incomplete decomposition of resistate minerals is the likely reason for the lack of agreement between methods using AR decomposition and total methods for Ba and Cr; the poorer relation between Co concentrations by AES_HF and AES_AR_P compared to the those between MS_HF and AES_AR_P may be due to differences in instrumental and matrix effects.

A greater number of partial methods were used to determine Cu, Ni, Pb, and Zn concentrations (table 3; figs. 5*B*, 6*B*, 7*B*, and 8*B*). Cu, Ni, Pb, and Zn concentrations determined by partial methods generally agree with those from of a total method and generally correspond to the 1-to-1 line; however, scatter is more prevalent at lower concentrations and is asymmetrically distributed below the 1-to-1 line (figs. 5*B*, 6*B*, 7*B*, and 8*B*). The low bias of the partial methods is most evident for low-range concentrations of Ni reported by the partial method AES_AR_P compared to those of total method AES_HF (fig. 6*B*). Ludington and others (2006) also reported increased scatter with a low bias at lower concentrations for As, Pb, Cd, Cu, Ag, and Zn by partial compared to total methods in samples for the northern Great Basin. They suggest that the presence of metals in silicate minerals that are not dissolved or are incompletely dissolved by the partial method are responsible for the asymmetry in scatter; however, differences in instrumental and matrix effects and (or) differences in the uncertainty of the left-censoring threshold cannot be ruled out because documentation of details of the methods is inadequate or nonexistent for most of the methods.

Semiquantitative Visual Six-Step Direct-Current Arc Emission Spectrography Compared to Total and Partial Methods

The ES_SQ method is a semiquantitative analytical method in which concentrations that fall within a specific interval are reported as the mid-point of that interval rather than as the actual value (table 1). Therefore, ES_SQ determinations are constrained to specific values and, consequently, appear as scatter at discrete intervals when plotted against the concentrations determined by a total or partial method (figs. 2*C*, 3*C*, 4*C*, 5*C*, 6*C*, 7*C*, and 8*C*). To assess whether the scatter would be expected due to the binned nature of the ES_SQ determinations, boxes sized to the ES_SQ concentrations range associated with the intervals are placed on the

10

1-to-1 line. Elemental concentrations determined by an alternate technique, here represented on the y-axis, that fall within the height of the box are within the expected scatter of the ES_SQ bin intervals; values that lie beyond the box height are outside the expected scatter.

When Ba, Co, Cr, Cu, Ni, Pb, and Zn concentrations determined by ES_SQ are compared to those determined by a total method that uses either a multi-acid method that includes HF or a sinter decomposition techniques, a general increase in the median concentrations of the total method typically is observed, but the scatter generally exceeds that expected for the ES_SQ binning intervals (figs. 2*C*, 3*C*, 4*C*, 5*C*, 6*C*, 7*C*, and 8*C*). The median values of the concentrations of Ba and Co determined by NA method with increasing ES_SQ bin also generally increase, but the scatter exceeds that expected for the ES_SQ intervals (figs. 2*C* and 3*C*). Only 48 of the 1,510 samples analyzed for Zn by ES_SQ and NA had detectable concentrations by both methods due to the high left-censoring thresholds for Zn by these methods (table 7) and comparison plots were not made. However, cursory evaluation of the 48 samples showed a general increase in the median of the NA values but scatter exceeded that expected. The Cr concentrations determined by ES_SQ do not agree with those of the NA method nor is there any agreement between the Pb concentrations determined by ES_SQ and those determined by the EDX method (Figure 7C).

Discussion

Data from sample reanalysis provide an opportunity to compare concentration data determined by different analytical methods on the same field sample. Shortcomings of the comparisons are that (1) the "true" concentration of an element is not known and only one measurement is available for each method, precluding statistical evaluation of the relative accuracy and precision of the analytical methods; and (2) no sample suite is common across the various method combinations. Consequently, different samples are represented in each plot. Because of these shortcomings, only qualitative observations can be made; nevertheless, evaluation of the paired analytical methods provides insight into data comparability.

Evaluation of the Best-Value Selection

The "best-values" concentration of the compiled dataset was used in the statewide mineral prospectivity evaluations (Karl and others, 2016). The best-values concept was introduced in AGDB2 to handle elements with multiple determinations in a single sample (Granitto and others, 2013). Because the best-value concentration is used in the mineral prospectivity analysis, scrutinizing its selection is important. The best values are selected from the different analytical results available for a sample by applying a hierarchical method-ranking scheme. The best-value rubric was designed for mineral assessment purposes and the rank of the methods was set by expert opinion (Granitto and others, 2013). Factors considered in developing the ranks included the (1) weight of the analyzed sample, method of decomposition of the sample during the preparation for analysis, (2) precision and accuracy of the instrument used in each method, (3) upper and lower limits of detection for a given element by a given method, (4) age of the method and stage of its development when a specific analysis was performed, and (5) analytical laboratory and equipment used (Granitto and others, 2013). The best value for an element in a sample was determined using the following criteria:

1. Lowest-rank assignments indicate the most preferred analytical method.
2. Concentrations greater than the lower detection limit are prioritized. Therefore, if the lowest-ranked (most preferred) method has a value less than the detection limit (that is, left-censored) for the element and a higher-ranked method has an analytic value that is not left-censored, the higher-ranked method is selected as the best-value method for that element in that sample.
3. Total methods are preferred over partial methods. However, a partial method may be selected as the best-value method for an element in a sample if the concentration of a given element by the total method is left-censored data.
4. If all analytic values by all methods are left-censored, selection of the best-value method is based on a separate censored value ranking. As with the uncensored ranking, lower ranked methods are the preferred method. Censored ranking principally is based on the method's lowest limit of detection [LLD].

The lowest ranked (preferred method) for Ba, Cr, Co, Cu, Ni, and Zn is NA (Granitto and others, 2013). Because the NURE program in Alaska used NA to analyze Ba, Cr, Co, and Zn, the best value for these elements in the combined dataset is always the original NURE-NA data unless the NURE concentration was left-censored (that is, less than the detection limit). This applies not only to NURE samples that also were analyzed by ES_SQ but to those reanalyzed under the USGS National Geochemical Survey project using the AES_HF method and those of the recent reanalysis efforts using a total method involving sinter digestion as well (Werdon and others, 2015a–e). For example, of the NURE samples that were reanalyzed under the USGS National Geochemical Survey project, more than 80 percent of the Ba, Co, and Cr best-value determinations and more than 40 percent of the Zn best-value determinations were original NURE concentrations; only those samples with left-censored NURE concentrations had a best-value determination that corresponded to the methods used during reanalysis. The high proportion of left-censored Zn data determined by the NURE program indicates the high censoring threshold of the NURE-NA method, which is the reason for the lower retention of the original NURE data as the best-value selection.

Given the age and the high uncertainty associated with the left-censoring threshold of the NURE-NA method, whether NA by NURE should outrank more modern analytical methods is arguable. Comparisons between the NURE-NA and AES_HF Cr concentration show extensive scatter that is asymmetric and primarily lies above the 1-to-1 line. Asymmetric scatter distributed above the 1-to-1 line also is seen in the comparisons of Cr concentrations determined by AES_HF to those determined by methods using a sinter or fusion decomposition technique. Taken together, these observations suggest that the AES_HF method does not fully digest some chromium-bearing minerals and the selection of the NURE-NA concentration as the best value is reasonable. In contrast, Ba, Co, and Zn concentrations determined by AES_HF correspond well with those determined by methods using a sinter and fusion decomposition technique. This suggests that most of the minerals containing Ba, Co, and Zn are adequately dissolved by the AES_HF method. This observation—coupled with the high uncertainty associated with the NURE-NA determinations of less than 1,500–3,000 ppm for Ba, 100–200 ppm for Cr, 20 ppm for Cu, and about 100 to 1,000 ppm for Zn—suggests that the NURE-NA method should not outrank the methods used by the USGS National Geochemical Survey project for the reanalysis of NURE samples for these elements.

Instrumental neutron activation analysis (NA) is the lowest-ranked method (that is, most preferred method) for most of the elements reported by the NURE program in Alaska, including Ce, Dy, and Eu. Consequently, when NURE samples are reanalyzed by most of the common multi-element packages, the NURE-NA method will be selected as the best-value determination. Because the NURE-NA method was designed for high throughput, the uncertainty associated with these determinations may be higher than those of other NA methods. The evaluation of paired data can aid the decision whether to retain the selection of the NURE-NA determination as the best-value determination of an element or to select a determination by an alternate method, if available. (Note: in the newly released Alaska Geochemical Database Version 3 (AGDB3 [Granitto, 2019], several instrumental neutron activation analysis techniques have been distinguished from one another; however, the NURE-NA method is still ranked lower than the other methods in AGDB3 for many elements including those detailed here.)

In contrast to NA, ES_SQ usually is the highest-ranked (least favorable) total method. Consequently, when multiple total determinations are available, ES_SQ will only be selected as the best value for a sample if the concentration by an alternate total method is left-censored. However, all total methods including ES_SQ are preferred to those of the partial methods in the best-value selection process. For elements commonly associated with resistant minerals, this selection rule is reasonable. For example, Ba concentrations determined by methods using AR digestion are biased low compared to NA and to total methods using a multi-acid or sinter digestion (fig. 2*B*). However, for elements residing in more soluble minerals, reconsideration of this selection is warranted. For example, Co concentrations determined by total methods MS_HF and NA and partial methods AES_AR_P and MS_AR_P agree reasonably well, as do Pb concentrations by several partial and total method combinations (figs. 3*B* and 7*B*). Even for Ni, which may be found in resistate minerals (for example, olivine), concentrations determined by AES_AR_P agree reasonably well with concentrations determined by total method AES_HF (fig. 6*B*). Given the considerable scatter in the ES_SQ data when compared to most total methods, the selection of a partial method—particularly one using an AR digestion—over the ES_SQ value would be reasonable for Co, Ni, and Pb.

Additionally, the preference for detected concentrations in the best-value selection should be carefully considered. This selection rule is reasonable when methods have similar detection limits with similar uncertainty. However, when the methods have different detection limits with different uncertainties, the selection may not be advisable. For example, ES_SQ was selected as the best-value method for Ni, Cu, and Cr for several samples because the corresponding AES_ST concentrations were censored. The AES_ST concentrations for Ni, Cu, and Cr were left-censored at less than 5 ppm in 87 samples for Ni and left-censored at less than 10 ppm in 76 samples for Cu and 64 samples for Cr. The corresponding ES_SQ concentrations, which for these samples are the best-value determination, ranged from 5 to 200 ppm for Ni, from 5 to 70 ppm for Cu, and from 10 to 150 ppm for Cr. Although for Ni, Cu, and Cr relatively few samples are affected, for other elements the effect may be more pronounced. Consequently, the ramifications of prioritizing detected values during the best-values selection process need to be understood, and the effects for the element of interest when using the best-values determination of the combined dataset need to be evaluated.

Finally, although changes to the best-value rubric may be desirable for certain elements, the compiled dataset remains a mixed-method dataset, and, therefore, the uncertainty due to differences in analytical methodology must be considered when the data are used in mineral prospectivity analysis.

Paired Comparisons and the Mineral Prospectivity Evaluations

During the mineral prospectivity evaluations, concentrations of select elements were ranked or scored based on whether the concentrations exceeded selected threshold values. Different strategies for determining the cutoff thresholds were used in the prospectivity analysis (Karl and others, 2016). To illustrate the possible effect of the analytical method on a sample's sediment geochemical score, dashed lines are shown at 1.5, 3.5, 7.5, and 15.5 times the element's background levels on figures 2–8 (background is defined as the median concentration in the statewide dataset; Lee and others, 2016). The interval between cutoff values that surrounds the 1-to-1 line is shaded pink and concentrations for the samples that fall outside the shaded boxes would be scored differently in a prospectivity analysis.

The difference between Ba, Co, Cr, Cu, Ni, Pb, and Zn concentrations determined by ES_SQ to those determined by other total methods is great enough that many samples would receive different scores depending on the selected method of analysis (figs. 2*C*, 3*C*, 4*C*, 5*C*, 6*C*, 7*C,* and 8*C*). For example, Pb concentrations determined by ES_SQ generally are higher than concentrations determined by the multi-acid or sinter methods (fig 7*C*). Consequently, these samples generally would receive a higher score for Pb determined by ES_SQ. At concentrations greater than 38.5 ppm (3.5 times background concentrations), Pb concentrations by all total and partial methods except EDX agree well enough that they would receive the same score using the multiples of background used in this example (fig.7*C*). The influence of ES_SQ on the prospectivity analysis could be reduced by selecting, if available, an alternative analysis including a partial method for the best-value method. For Pb, partial methods are the most commonly available alternative to a best-value selection of ES_SQ. However, because of the limited distribution, the effect of this reselection will be regional rather than statewide. Substitution of partial methods for ES_SQ would not be advisable for Ba and Cr given the lack of agreement between the partial and total methods and the common occurrence of these elements in resistant minerals. In addition to method substitution, ES_SQ determinations could be scored separately using broader cutoffs (see platinum group element evaluation in Karl and others, 2016), or an uncertainty measure associated with the geochemical method could be introduced in the prospectivity evaluations.

Selection of AES_HF as the preferred method over the NURE-NA and EDX methods is a possibility for several elements. The better correlation between the AES_HF and sinter methods and the likelihood that the NURE methods have greater uncertainty than the AES_HF at the lower concentrations suggests that substitution of the AES_HF determinations is warranted for Ba, Co, Cu, Pb, and Zn. This substitution may have a greater effect on a statewide prospectivity analyses than the substitution for ES_SQ because of the statewide distribution of samples but will not remove all NURE-derived NA and EDX determinations from the compiled dataset. If the scoring limits are high enough, NA or EDX could be combined with the other total methods. Alternatively, they could be scored separately, or an uncertainty criterion could be introduced.

Summary

The dataset used in the USGS mineral prospectivity analyses is a compilation of sediment geochemical data that were collected over several decades. Because of the variety of analytical methods used to determine the concentrations of many of the elements, evaluation of the concentration data is an important step in a mineral prospectivity analysis. Considerations for data evaluation include the scale of analysis (statewide or regional), the coverage of data

14

produced by a particular method, and the performance of alternative methods, if available. Data handling options include:

1. Using the analytical values associated with the best-value method without differentiating among the methods;
2. Differentiating among the methods, for example, by using separate scoring or certainty criteria for different methods;
3. Eliminating analyses by certain methods (this may considerably affect sample distribution); or
4. Selecting a value determined by a method other than the best-value method. However, reselection will not necessarily replace all analyses by the "problematic" best method in the dataset.

Evaluation of the paired analyses for barium (Ba), cobalt (Co), chromium (Cr), copper (Cu), nickel (Ni), lead (Pb), and zinc (Zn) indicates that quantitative analytical methods can be grouped based on their sample decomposition class (for example, total or partial) but the semiquantitative emission spectrographic method should be handled separately in the mineral prospectivity analysis. Generally, agreement is reasonable between concentrations determined by quantitative total methods for Ba, Co, Cu, Ni, Pb, and Zn. However, Cr values are lower from methods using a multi-acid dissolution that included hydrofluoric acid (HF) than for methods that use a sinter or fusion decomposition. Poor recovery of Cr in silicate minerals may be responsible for the lower concentrations following the multi-acid dissolution. Additionally, considerable scatter occurs at low- to middle-range concentrations of Ba, Co, Cr, Cu, Pb, Ni, and Zn determined by the National Uranium Resource Evaluation (NURE) program's instrumental neuron activation analysis (NA) and energy-dispersive x-ray spectroscopy (EDX) methods compared to the method using atomic emission spectrometry after digestion with HF-HCl-HNO3-HClO4 (AES_HF). The extensive scatter may relate, in part, to differences in the uncertainty of the methods for this concentration range. Review of the documentation for the method suggests that uncertainty is greater associated with the NURE-NA and NURE-EDX analyses than with the AES_HF analysis at low- to middle-range elemental concentrations. The difference in analytic values yielded by the different methods is enough that it could affect the prospectivity analysis. Reselection of AES_HF over NURE-NA and NURE-EDX methods is a possibility, or scoring cutoffs should be set high enough to accommodate the lack of sensitivity.

Comparisons of the concentrations determined by total and partial methods typically show general agreement for Co, Cu, Ni, Pb, and Zn. However, poor agreement was found for Ba and Cr. Incomplete decomposition of minerals containing these elements is likely the reason for the lack of agreement. Comparisons between semiquantitative visual six-step direct-current arc emission spectrography (ES_SQ) and total or partial methods usually have general correspondence in samples that have comparative concentrations. However, scatter between the paired analyses typically is beyond that expected from the range of values that a binned ES_SQ value represents and is enough to affect prospectivity analyses. Consequently, ES_SQ determinations should be handled separately from quantitative methods.

References Cited

Baedecker, P.A., and Mckown, D.M., 1987, Instrumental neutron activation analysis of geochemical samples, *in* Baedecker, P.A., ed., Methods for geochemical analysis: U.S. Geological Survey Bulletin 1770, p. H1-H14, accessed February 28, 2018, at https://pubs.usgs.gov/bul/1770/report.pdf.

Boliver, S.L., 1987, The Los Alamos Scientific Laboratory approach to hydrogeochemical and stream sediment reconnaissance for uranium in the United States: Los Alamos Scientific Laboratory, LA-8691-MS, 22p.

Briggs, P.H., 2002, The determination of forty elements in geological and botanical samples by inductively coupled plasma-atomic emission spectrometry, chap. G *of* Taggart, J.E., Jr., ed., Analytical methods for chemical analysis of geologic and other materials, U.S. Geological Survey: U.S. Geological Survey Open-File Report 02-223, p. G–1G-18.

Chao, T.T, 1984, Use of partial dissolution techniques in geochemical exploration: Journal of Geochemical Exploration, v. 20, p. 101–135.

Chao, T.T., and Sanzolone, R.F., 1992, Decomposition techniques: Journal of Geochemical Exploration, v. 44, p. 65–106.

Church, S.E., Mosier, E.L., and Motooka, J.M, 1987, Mineralogical basis for the interpretation of multi-element (ICP-AES), oxalic acid, and aqua regia partial digestions of stream sediments for reconnaissance exploration geochemistry: Journal of Geochemical Exploration, v. 29, p. 207–233.

Golightly, D.W., Dorrzapf, A.F., Mays, R.E., Fries, T.L., and Conklin, N.M., 1987, Analysis of geologic materials by direct-current arc emission spectrography and spectrometry, *in* Baedecker, P.A., ed., Methods for geochemical analysis: U.S. Geological Survey Bulletin 1770, p. A1–A13, accessed February 28, 2018, at https://pubs.usgs.gov/bul/1770/report.pdf.

Granitto, M., Schmidt, J.M., Shew, N.B., Gamble, B.M., and Labay, K.A., 2011, Alaska geochemical database (AGDB)—Geochemical data for rock, sediment, soil, mineral, and concentrate sample media: U.S. Geological Survey Data Series 637, 39 p. pamphlet and database, 1 DVD, accessed January 3, 2018, at https://doi.or/10.3133/ds63.

Granitto, M., Schmidt, J.M., Shew, N.B., Gamble, B.M., and Labay, K.A., 2013, Alaska geochemical database, version 2.0 (AGDB2)—Including "best value" data compilations for rock, sediment, soil, mineral, and concentrate sample media: U.S. Geological Survey Data Series 759, 20 p., 1 DVD, accessed January 3, 2018, at https://pubs.er.usgs.gov/publication/ds759.

Granitto, M, Shew, N.B., Karl, S.M., Wang, B., Labay, K.A., Werdon, M.B., Hoppe, J., and Seitz, S., 2019, Alaska Geochemical Database, version 3.0 (AGDB3)—Including "best value" data compilations for rock, sediment, soil, mineral, and concentrate sample media: U.S. Geological Survey Data Series 1117, 33 p., accessed September 2019, at https://doi.org/10.3133/ds1117.

Grimes, D.J., and Marranzino, A.P., 1968, Direct-current arc and alternating-current spark emission spectrographic field methods for the semiquantitative analysis of geologic materials: U.S. Geological Survey Circular 591, 6 p., accessed February 28, 2018, at https://pubs.usgs.gov/circ/1968/0591/report.pdf.

Hansel, J.M., and Martell, C.J., 1977, Automated energy-dispersive x-ray determination of trace elements in stream sediment: Los Alamos Scientific Laboratory informal report LA-6869-MS, 8 p.

Information Systems Programs Energy Resources Institute, 1985, A technical history of the hydrogeochemical and stream sediment reconnaissance (HSSR) programs of the National Uranium Resource Evaluation (NURE) 1973–1984: Produced for the U.S. Department of Energy, 66 p., accessed February 28, 2018, at https://pubs.usgs.gov/of/1997/ofr-97-0492/nurepubs.htm.

Johnson, R.G., and King, B.-S.L., 1987, Energy-dispersive x-ray fluorescence spectrometry, *in* Baedecker, P.A., ed., Methods for geochemical analysis: U.S. Geological Survey Bulletin 1770, p. F1–F5, accessed February 28, 2018, at https://pubs.usgs.gov/bul/1770/report.pdf.

Karl, S.M., Jones, J.V., III, and Hayes, T.S., eds., 2016, GIS-based identification of areas that have resource potential for critical minerals in six selected groups of deposit types in Alaska: U.S. Geological Survey Open-File Report 2016–1191, 99 p., 5 appendixes, 12 plates, scale 1:10,500,000, accessed February 28, 2018, at http://dx.doi.org/10.3133/ofr20161191.

Lee, G.K., Yager, D.B., Mauk, J.L, Granitto, M., Denning, P.D., Wang, B., and Werdon, M.B., 2016, The geochemical atlas of Alaska, 2016: U.S. Geological Survey Data Series 908, 25 p., 272 sheets (11"× 17"), GIS database, accessed February 28, 2018, at http://dx.doi.org/10.3133/ds908.

Lichte, F.E., Golightly, D.W., and Lamothe, P.J., 1987, Inductively coupled plasma-atomic emission spectrometry, *in* Baedecker, P.A., ed., Methods for geochemical analysis: U.S. Geological Survey Bulletin 1770, p. B1–B10, accessed February 28, 2018, at https://pubs.usgs.gov/bul/1770/report.pdf.

Ludington, S., Folger, H., Kotlyer, B., Mossotti, V.G., Coomb, M.J., and Hidnenbrand, T.G., 2006, Regional surficial geochemistry of the northern Great Basin: Economic Geology, v. 101, pp. 33–57.

McKown, D.M., and Millard, H.T., 1987, Determination of uranium and thorium by delayed neutron counting, *in* Baedecker, P.A., ed., Methods for geochemical analysis: U.S. Geological Survey Bulletin 1770, p. I1–I12, accessed February 28, 2018, at https://pubs.usgs.gov/bul/1770/report.pdf.

Minor, M.M, Hensley, W.K., Denton, M.M., and Garcia, S.R., 1982, An automated activation analysis system: Journal of Radioanalytical Chemistry, v. 70, nos. 1–2, p. 459–471.

Motooka, J.M., and Grimes, D.J., 1976, Analytical precision of one-sixth order semiquantitative spectrographic analysis: U.S. Geological Survey Circular 738, 25 p., accessed February 28, 2018, at https://pubs.usgs.gov/circ/1976/0738/report.pdf.

Myers, A.T., Havens, R.G., and Dunton, P.J., 1961, A spectrochemical method for the semiquantitative analysis of rocks, minerals and ores: Geological Survey Bulletin 1084-I, p. 207–229, accessed February 28, 2018, at https://pubs.usgs.gov/bul/1084i/report.pdf.

Nunes, H.P., and Weaver, T.A., 1978, Hydrogeochemical and stream sediment reconnaissance of the National Uranium Resource Evaluation Program, July–September 1977: Los Alamos, New Mexico, Los Alamos Scientific Laboratory, LA-6993-PR, 14 p.

Potts, P.J., 1992, A handbook of silicate rock analysis: New York, Springer Science+Business Media, 631 p.

Taggart, J.E., Jr., ed., 2002, Analytical methods for chemical analysis of geologic and other materials, U.S. Geological Survey: U.S. Geological Survey Open-File Report 02-223, p. vi–xi.

Taggart, J.E., Jr., Lindsay, J.R., Scott, B.A., Vivit, D.V., Bartel, A.J., and Stewart, K.C., 1987, Analysis of geologic materials by wavelength-dispersive x-ray fluorescence spectrometry, *in* Baedecker, P.A., ed., Methods for geochemical analysis: U.S. Geological Survey Bulletin 1770, p. E1–E19, accessed February 28, 2018, at https://pubs.usgs.gov/bul/1770/report.pdf.

U.S. Geological Survey, 2008, The National Geochemical Survey—Database and documentation: U.S. Geological Survey Open-File Report 2004-1001, accessed February 28, 2018, at https://mrdata.usgs.gov/geochem/doc/home.htm.

Werdon, M.B., Azain, J.S., and Granitto, M., 2014, Reanalysis of historical U.S. Geological Survey sediment samples for geochemical data from the western part of the Wrangellia terrane, Anchorage, Gulkana, Healy, Mt. Hayes, Nabesna and Talkeetna Mountains quadrangles, Alaska: State of Alaska Department of Natural Resources, Division of Geological and Geophysical Surveys, Raw-Data File 2014-5.

Werdon, M.B., Granitto, M., and Azain, J.S., 2015a, Geochemical reanalysis of historical U.S. Geological Survey sediment samples from the Haines Area, Juneau and Skagway quadrangles, southeast Alaska: State of Alaska Department of Natural Resources, Division of Geological and Geophysical Surveys, Raw-Data File 2015-5.

Werdon, M.B., Granitto, M., and Azain, J.S., 2015b, Geochemical reanalysis of historical U.S. Geological Survey sediment samples from the Immachuk, Kugruk, Kiwalik, and Koyuk River drainages, Granite Mountain, and the northern Darby Mountains, Bendeleben, Candle, Kotzebue, and Solomon quadrangles, Alaska: State of Alaska Department of Natural Resources, Division of Geological and Geophysical Surveys, Raw-Data File 2015-4.

Werdon, M.B., Granitto, M., and Azain, J.S., 2015c, Geochemical reanalysis of historical U.S. Geological Survey sediment samples from the Kougarok area, Bendeleben and Teller quadrangles, Seward Peninsula, Alaska: State of Alaska Department of Natural Resources, Division of Geological and Geophysical Surveys, Raw-Data File 2015-6.

Werdon, M.B., Granitto, M., and Azain, J.S., 2015d, Geochemical reanalysis of historical U.S. Geological Survey sediment samples from the northeastern Alaska Range, Healy, Mount Hayes, Nabesna, and Tanacross quadrangles, Alaska: State of Alaska Department of Natural Resources, Division of Geological and Geophysical Surveys, Raw-Data File 2015-7.

Werdon, M.B., Granitto, M., and Azain, J.S., 2015e, Geochemical reanalysis of historical U.S. Geological Survey sediment samples from the Tonsina area, Valdez quadrangle, Alaska: State of Alaska Department of Natural Resources, Division of Geological and Geophysical Surveys, Raw-data File 2015-8.

Yokoyama, T., Makishima, A., and Nakamura, E., 1999, Evaluation of the coprecipitation of incompatible trace elements with fluoride during silicate rock dissolution by acid digestion: Chemical Geology, v. 157, p. 175–187.

Figures

In the multi-part, multi-page figures that follow, figure captions appear on last page of each figure as noted here:

- Figure 2 caption on p. 22.
- Figure 3 caption on p. 25.
- Figure 4 caption on p. 28.
- Figure 5 caption on p. 32.
- Figure 6 caption on p. 35.
- Figure 7 caption on p. 39.
- Figure 8 caption on p. 43.
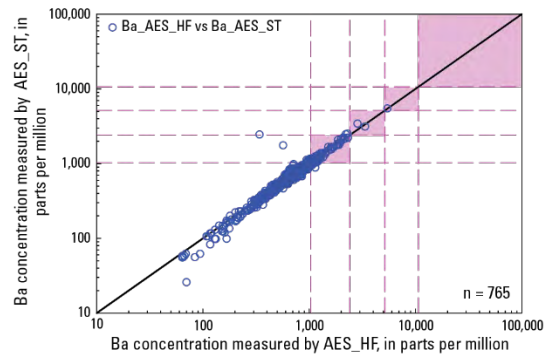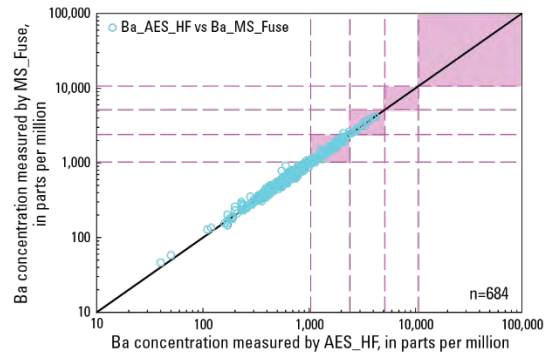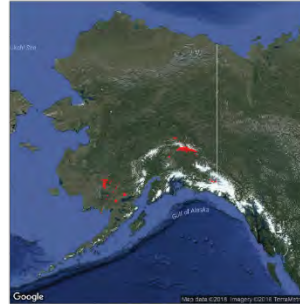
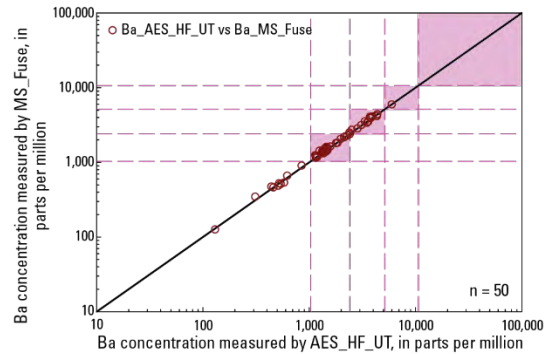### *A.* Barium total to total

Ba by AES_HF and NA

Ba by AES_HF and AES_ST

Ba by AES_HF and MS_Fuse

Ba by AES_HF_UT and MS_Fuse

EXPLANATION:

Scatter tolerance for scoring based on the multiples of background

Lines corresponding to 1.5, 3.5, 7.5, and 15.5 times the background concentration for Alaska

One-to-one line

n = 5,374 Number of uncensored pairs

20

B. Barium total to partial

Ba by AES_HF and AES_AR_P

Ba by AES_ST and AES_AR_P

Ba by NA and AES_AR_P

Ba by NA and MS_AR_P

EXPLANATION:

- Scatter tolerance for scoring based on the multiples of background
- Lines corresponding to 1.5, 3.5, 7.5, and 15.5 times the background concentration for Alaska
- One-to-one line
- n = 1,600 Number of uncensored pairs

C. Barium ES_SQ to total

Figure 2. Graphs showing comparison of uncensored paired analytical values for barium (Ba) (*A*) by two analytical methods with total decomposition of the sample; (*B*) by two analytical methods, one with a total decomposition of the sample and the other with a partial decomposition of the sample; and (*C*) by semiquantitative visual six-step direct-current arc emission spectrography and an analytical method with total decomposition of the sample; and images showing spatial distribution of sample in each analysis category in Alaska. On all graphs, n is the number of uncensored pairs. Small green boxes denote the expected range of scatter for the semiquantitative emission spectrographic (ES_SQ) technique. Pink dashed lines indicate 1.5, 3.5, 7.5, and 15.5 times the background concentration (Lee and others, 2016) of the depicted element and represent possible cutoff values for the geochemical scoring procedure during the prospectivity analysis. Samples that fall within the pink rectangular shaded regions would receive the same score in the mineral prospectively analysis (Karl and others, 2016).
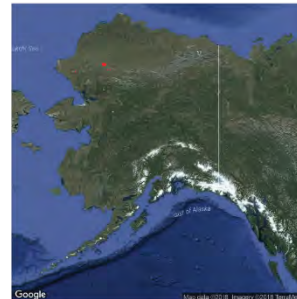
A. **Cobalt total to total**

Co by AES_HF and NA

Co by MS_HF and AES_HF

Co by MS_ST and MS_HF

Co by MS_ST and AES_HF

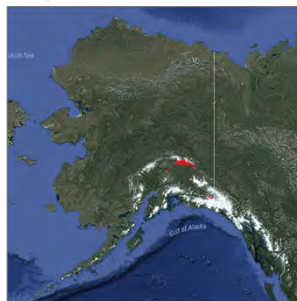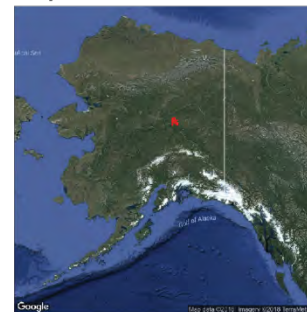**EXPLANATION:**

Scatter tolerance for scoring based on the multiples of background

Lines corresponding to 1.5, 3.5, 7.5, and 15.5 times the background concentration for Alaska

One-to-one line

n = 5,561 Number of uncensored pairs

23

B. Cobalt total to partial

Co by AES_HF and AES_AR_P

Co by MS_HF and AES_AR_P

Co by NA and AES_AR_P

Co by NA and AES_AR_P

EXPLANATION:

Scatter tolerance for scoring based on the multiples of background

Lines corresponding to 1.5, 3.5, 7.5, and 15.5 times the background concentration for Alaska

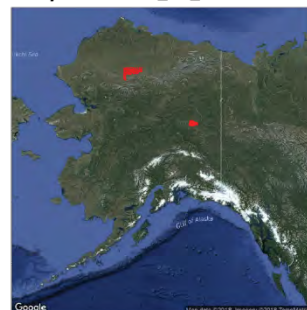One-to-one line

n = 270   Number of uncensored pairs

Figure 3. Graphs showing comparison of uncensored paired analytical values for cobalt (Co) (*A*) by two analytical methods with total decomposition of the sample; (*B*) by two analytical methods, one with a total decomposition of the sample and the other with a partial decomposition of the sample; and (*C*) by semiquantitative visual six-step direct-current arc emission spectrography and an analytical method with total decomposition of the sample; and images showing spatial distribution of sample in each analysis category in Alaska. See figure 2 for a complete explanation.

A. Chromium total to total

Cr by AES_HF and NA

Cr by AES_HF and AES_ST

Cr by AES_HF and MS_Fuse

Cr by AES_HF_UT and MS_Fuse

EXPLANATION

Scatter tolerance for scoring based on the multiples of background

Lines corresponding to 1.5, 3.5, 7.5, and 15.5 times the background concentration for Alaska

One-to-one line

n = 5,608   Number of uncensored pairs

B. Chromium total to partial
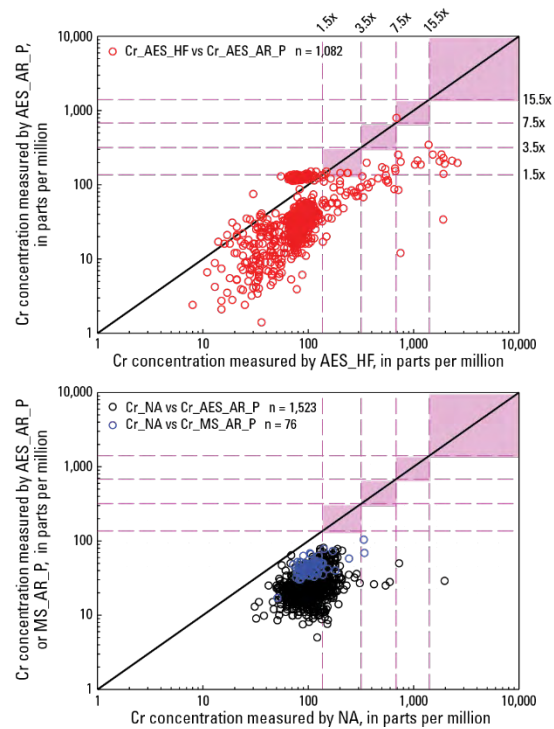
Cr by AES_HF and AES_AR_P

Cr by NA and AES_AR_P

Cr by NA and MS_AR_P

EXPLANATION

Scatter tolerance for scoring based on the multiples of background

Lines corresponding to 1.5, 3.5, 7.5, and 15.5 times the background concentration for Alaska

One-to-one line

n = 1,082 Number of uncensored pairs

C. Chromium ES_SQ to total

Figure 4. Graphs showing comparison of uncensored paired analytical values for chromium (Cr) (*A*) by two analytical methods with total decomposition of the sample; (*B*) by two analytical methods, one with a total decomposition of the sample and the other with a partial decomposition of the sample; and (*C*) by semiquantitative visual six-step direct-current arc emission spectrography and an analytical method with total decomposition of the sample; and images showing spatial distribution of sample in each analysis category in Alaska. See figure 2 for a complete explanation.

A. Copper total to total
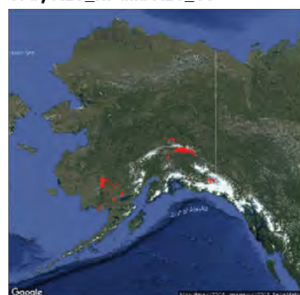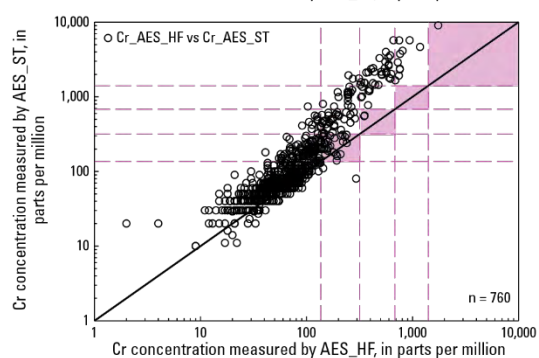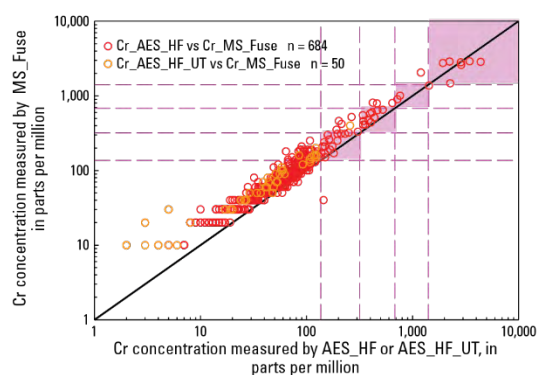

Cu_AES_HF vs Cu_EDX (NURE)

1.5x 3.5x 7.5x 15.5x

15.5x
7.5x
3.5x
1.5x

Cu concentration measured by EDX, in parts per million

Cu concentration measured by AES_HF, in parts per million

n = 4,627

Cu_AES_HF vs Cu_AES_ST

Cu concentration measured by AES_HF, in parts per million

Cu concentration measured by AES_ST, in parts per million

n = 724

Cu by AES_HF and EDX
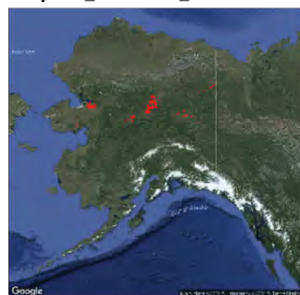

Cu by AES_ST and AES_HF

EXPLANATION:

Scatter tolerance for scoring based on the multiples of background

Lines corresponding to 1.5, 3.5, 7.5, and 15.5 times the background concentration for Alaska
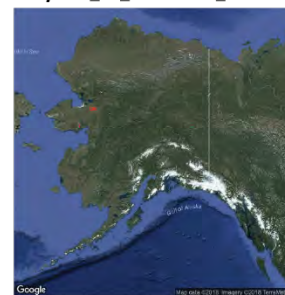
One-to-one line

n = 4,627 Number of uncensored pairs

29

B. Copper total to partial

EXPLANATION:

███ Scatter tolerance for scoring based on the multiples of background

– – – Lines corresponding to 1.5, 3.5, 7.5, and 15.5 times the background concentration for Alaska

——— One-to-one line

n = 4,627 Number of uncensored pairs

Cu by AES_HF and AES_AR_P


Cu by AES_HF and AA_F_AR_P
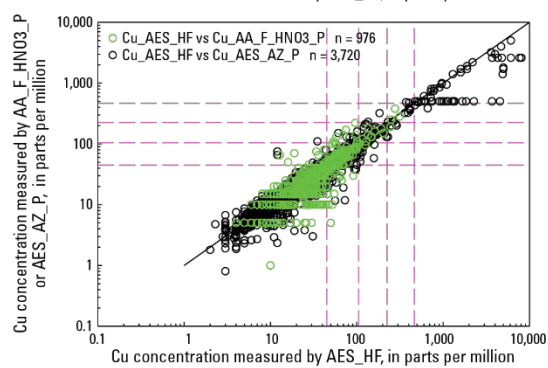
Cu by AES_HF and AES_AZ_P

Cu by AES_HF and AA_F_HNO3_P

Cu by EDX and AES_AR_P

Cu by EDX and AES_AZ_P

Cu by EDX and MS_AR_P

30

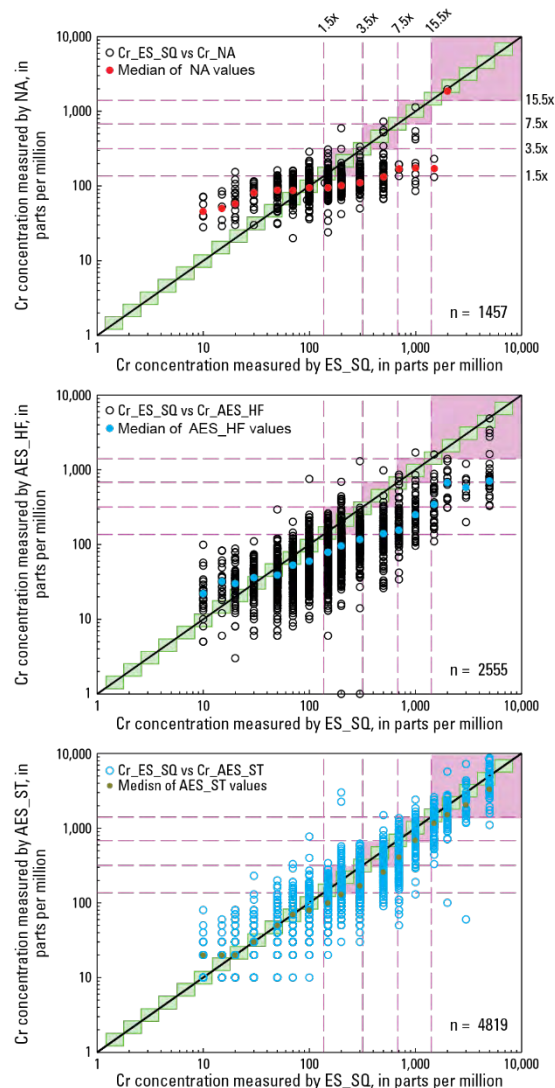*B*. Copper total to partial—Continued

Cu by AES_ST and AA_F_HNO3_P

Cu by AES_ST and AES_AZ_P

EXPLANATION:

Scatter tolerance for scoring based on the multiples of background

Lines corresponding to 1.5, 3.5, 7.5, and 15.5 times the background concentration for Alaska

One-to-one line

n = 4,627 Number of uncensored pairs

Figure 5. Graphs showing comparison of uncensored paired analytical values for copper (Cu) (*A*) by two analytical methods with total decomposition of the sample; (*B*) by two analytical methods, one with a total decomposition of the sample and the other with a partial decomposition of the sample; and (*C*) by semiquantitative visual six-step direct-current arc emission spectrography and an analytical method with total decomposition of the sample; and images showing spatial distribution of sample in each analysis category in Alaska. See figure 2 for a complete explanation.
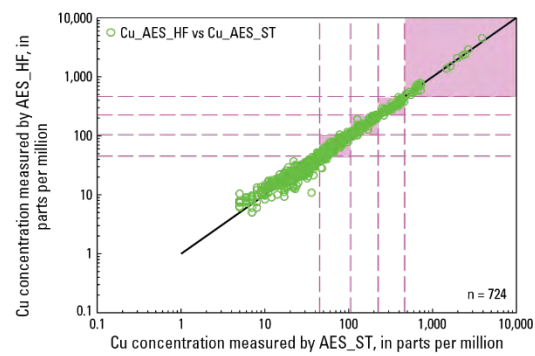
A. Nickel total to total

Ni by AES_HF and EDX

Ni by AES_HF and AES_ST

Ni by AES_HF and NA

EXPLANATION:

Scatter tolerance for scoring based on the multiples of background

Lines corresponding to 1.5, 3.5, 7.5, and 15.5 times the background concentration for Alaska

One-to-one line

n = 3,926 Number of uncensored pairs

B. Nickel total to partial

Ni by AES_HF and AES_AR_P
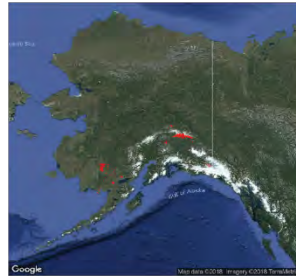
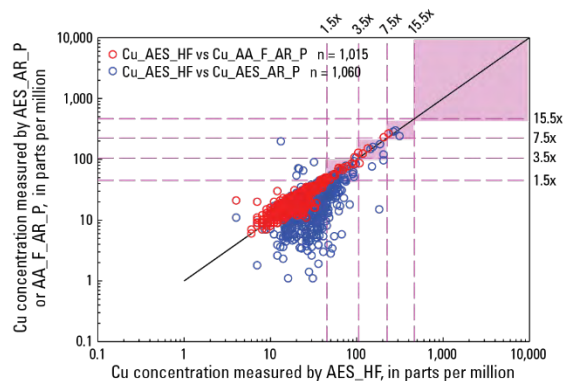Ni by AES_ST and AA_F_HNO3_P

Ni by NA and AES_AR_P

EXPLANATION:

Scatter tolerance for scoring based on the multiples of background

Lines corresponding to 1.5, 3.5, 7.5, and 15.5 times the background concentration for Alaska

One-to-one line

n = 1,155 Number of uncensored pairs

Ni by EDX and MS_AR_P

Ni by EDX and AES_AR_P

34

Figure 6. Graphs showing comparison of uncensored paired analytical values for nickel (Ni) (*A*) by two analytical methods with total decomposition of the sample; (*B*) by two analytical methods, one with a total decomposition of the sample and the other with a partial decomposition of the sample; and (*C*) by semiquantitative visual six-step direct-current arc emission spectrography and an analytical method with total decomposition of the sample; and images showing spatial distribution of sample in each analysis category in Alaska. See figure 2 for a complete explanation

A. Lead total to total

Pb by AES_HF and EDX

Pb by MS_HF and MS_ST

Pb by AES_HF and MS_ST

Pb by MS_HF and AES_HF

EXPLANATION:

Scatter tolerance for scoring based on the multiples of background

Lines corresponding to 1.5, 3.5, 7.5, and 15.5 times the background concentration for Alaska

One-to-one line
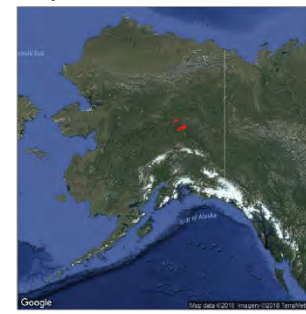
n = 2,802 Number of uncensored pairs

36

B. Lead total to partial

EXPLANATION:

 Scatter tolerance for scoring based on the multiples of background

— — Lines corresponding to 1.5, 3.5, 7.5, and 15.5 times the background concentration for Alaska

—— One-to-one line

n = 2,587 Number of uncensored pairs

Pb by AES_HF and AA_F_AR_P

Pb by AES_HF and AES_AR_P

Pb by AES_HF and AA_F_HNO3_P

Pb by AES_HF and AES_AZ_P

Pb by MS_HF and AA_F_AR_P

Pb by MS_HF and AES_AZ_P

37

B. Lead total to partial—Continued

Pb by MS_ST and AA_F_HNO3_P

Pb by MS_ST and AES_AZ_P

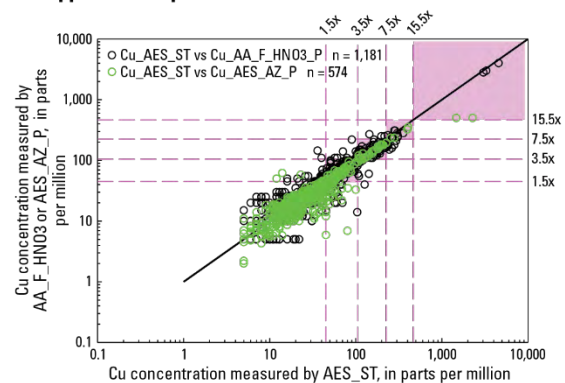**Pb by AES_AR_P and EDX**

Pb by AES_AZ_P and EDX

Pb by MS_AR_P and EDX

EXPLANATION:

Scatter tolerance for scoring based on the multiples of background

Lines corresponding to 1.5, 3.5, 7.5, and 15.5 times the background concentration for Alaska

One-to-one line

n = 2,587 Number of uncensored pairs

Figure 7. Graphs showing comparison of uncensored paired analytical values for lead (Pb) (*A*) by two analytical methods with total decomposition of the sample; (*B*) by two analytical methods, one with a total decomposition of the sample and the other with a partial decomposition of the sample; and (*C*) by semiquantitative visual six-step direct-current arc emission spectrography and an analytical method with total decomposition of the sample; and images showing spatial distribution of sample in each analysis category in Alaska. See figure 2 for complete explanation.

39

A. Zinc total to total

Zn by AES_HF and NA

Zn by AES_HF and AES_ST

EXPLANATION:

Scatter tolerance for scoring based on the multiples of background

Lines corresponding to 1.5, 3.5, 7.5, and 15.5 times the background concentration for Alaska

One-to-one line

n = 2,258 Number of uncensored pairs

B. Zinc total to partial

EXPLANATION:

Scatter tolerance for scoring based on the multiples of background

Lines corresponding to 1.5, 3.5, 7.5, and 15.5 times the background concentration for Alaska

One-to-one line

n = 2,258 Number of uncensored pairs

Zn by AES_HF and AA_F_HNO3_P

Zn by AES_HF and AES_AZ_P

Zn by AES_HF and AA_F_AZ_H2O2_P

Zn by AES_HF and AES_AR_P

Zn by AES_HF and AA_F_AR_P

Zn by AES_ST and AA_F_HNO3_P

Zn by AES_ST and AA_F_AZ_FUSE_P

41

B. Zinc total to partial—Continued

Zn by AES_ST and AES_AZ_P

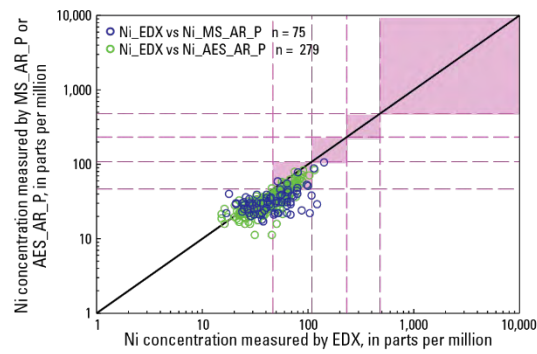Zn by AES_ST and AA_F_AZ_H2O2_P

Zn by NA and AES_AR_P

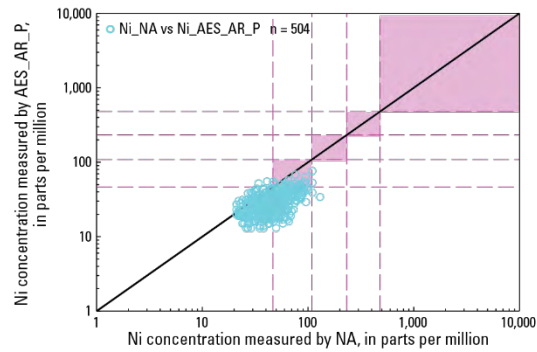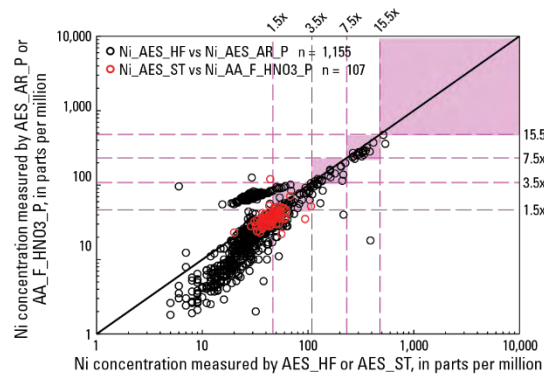Zn by NA and AES_AZ_P

EXPLANATION:

Scatter tolerance for scoring based on the multiples of background

Lines corresponding to 1.5, 3.5, 7.5, and 15.5 times the background concentration for Alaska

One-to-one line

n = 172   Number of uncensored pairs

Figure 8. Graphs showing comparison of uncensored paired analytical values for zinc (Zn) (*A*) by two analytical methods with total decomposition of the sample; (*B*) by two analytical methods, one with a total decomposition of the sample and the other with a partial decomposition of the sample; and (*C*) by semiquantitative visual six-step direct-current arc emission spectrography and an analytical method with total decomposition of the sample; and images showing spatial distribution of sample in each analysis category in Alaska. See figure 2 for a complete explanation.

Figure 9. Graphs showing distribution of the left-censoring thresholds found for barium (Ba; top left), cobalt (Co; bottom left), chromium (Cr; top right), and zinc (Zn; bottom right) for the instrumental neutron activation analysis used during the National Uranium Resource Evaluation (NURE) program in Alaska. NA, major and minor elements by long or short count instrumental neutron activation analysis.

Tables

Table 2. Number of Alaskan samples analyzed, left-censored data characteristics, and non-censored data characteristics for analytical methods with total decomposition of the sample used to determine barium (Ba), chromium (Cr), cobalt (Co), copper (Cu), nickel (Ni), lead (Pb), and zinc (Zn) concentrations.

[See section, "Method Abbreviations" for descriptions of method abbreviations used in the Method column. **Numsamples**: Total number of samples. **NumLCC**: Number of samples with left-censored concentrations. **minLCT:** Lowest left-censored threshold. **modeLCT:** Mode of the left-censored threshold. **maxLCT:** Highest left-censored threshold. **NumNCC:** Number of non-censored concentrations. **minNCC**: Minimum non-censored concentration. **modeNCC:** Mode of the non-censored concentrations. **maxNCC:** Maximum of the non-censored concentrations. **Abbreviation and symbols:** nd, not determined; <, less than; >, greater than]

Method	Numsamples	NumLCC	minLCT	modeLCT	maxLCT	NumNCC	minNCC	modeNCC	maxNCC
Ba summary									
AES_HF	14,153	0	nd	nd	nd	14,153	5	1,100	16,100
NA	69,252	8,259	<10	<100	<9,120	60,993	3	600	400,000
EDX	335	12	<20	<20	<20	323	20	540	584,000
MS_HF	522	0	nd	nd	nd	522	4	1,100	2,890
AES_Fuse	26	0	nd	nd	nd	26	24	34	9,100
MS_Fuse	734	0	nd	nd	nd	734	46.2	790	5,960
AES_HF_UT	50	0	nd	nd	nd	50	130	1,160	5,990
AES_ST	58,92	0	nd	nd	nd	5,892	2	1070	>10,000
WDX_Fuse	61	0	nd	nd	nd	61	610	740	990

Method	Numsamples	NumLCC	minLCT	modeLCT	maxLCT	NumNCC	minNCC	modeNCC	maxNCC
				Cr summary					
AES_HF	14,287	14	<1	<2	<5	14,273	1	79	12,000
NA	65,938	3,841	<1	<10	<214	62,097	1	90	14,550
MS_HF	522	0	nd	nd	nd	522	3.4	110	7,660
MS_Fuse	738	0	nd	nd	nd	738	10	80	2,900
AES_HF_UT	50	0	nd	nd	nd	50	2	3	258
AES_ST	5,892	194	<10	<10	<10	5,698	10	70	19,800
AES_Fuse	22	0	nd	nd	nd	22	33	59	395
WDX_Fuse	309	202	<27	<270	<480	107	68.4	340	1,300
				Co summary					
MS_HF	3,468	1	<1	<1	<1	3,467	0.2	12.6	391
NA	65,803	2,979	<0.1	<0.1	<11.7	62,824	0.7	13	999.9
AES_HF	11,482	66	<1	<2	<2	11,416	0.5	13	820
MS_Fuse	36	0	nd	nd	nd	36	5	13.5	37
MS_ST	5,892	6	<0.5	<0.5	<0.5	5,886	0.5	12.3	1,140
				Cu summary					
AES_HF	14,161	106	<1	<2	<2	14,055	1	15	35,000
NA	54	5	<1	<1	<1	49	1	3	53
MS_HF	706	0	nd	nd	nd	706	1	20	52,300
EDX	62,098	2,538	<7	<10	<10	59,560	7	24	13,863
MS_Fuse	4	0	nd	nd	nd	4	40	50	110
AES_ST	5,892	159	<5	<5	<5	5,733	5	16	4,570
AA_F_HF	21	0	nd	nd	nd	21	17	21	100
				Ni summary					
AES_HF	14,161	82	<1	<3	<5	14,079	0	28	2,100
NA	3,589	2,473	<20	<200	<200	1,116	21	200	4,800
MS_HF	706	2	<1	<2	<2	704	1	34	1,150
EDX	62,098	12,071	<10	<15	<15	50,027	9	27	1,830
MS_Fuse	4	0	nd	nd	nd	4	40	50	50
AES_ST	5,888	100	<5	<5	<5	5,788	5	42	1,950

46

Method	Numsamples	NumLCC	minLCT	modeLCT	maxLCT	NumNCC	minNCC	modeNCC	maxNCC
				Pb summary					
MS_HF	3,468	1	<1	<1	<1	3,467	0.7	12	19,900
AES_HF	11,490	563	<2	<4	<20	10,927	0.5	16	2,980
NA	54	1	<5	<5	<5	53	8	16	38
EDX	62,099	26,172	<5	<5	<5	35,927	4	5	63,081
MS_Fuse	4	0	nd	nd	nd	4	6	6	15
MS_ST	5,892	260	<5	<5	<5	5,632	5	10	>50,000
AA_F_HF	21	3	<5	<5	<5	18	10	50	150
				Zn summary					
AES_HF	14,296	3	<2	<2	<4	14,293	3	110	16,000
NA	66,699	35,027	<1	<200	<4,805	31,672	14	137	8,400
MS_HF	522	0	nd	nd	nd	522	16	140	40,100
MS_Fuse	4	0	nd	nd	nd	4	80	110	120
AES_HF_UT	50	0	nd	nd	nd	50	5	18	185
AES_ST	5,892	2	<5	<5	<5	5,890	11	89	>50,000
AA_F_HF	298	1	<5	<5	<5	297	30	100	1,000

Table 3. Number of Alaskan samples analyzed, left-censored data characteristics, and non-censored data characteristics for the partial decomposition of the sample used to determine barium (Ba), chromium (Cr), cobalt (Co), copper (Cu), nickel (Ni), lead (Pb), and zinc (Zn) concentrations.

[See section, "Method Abbreviations" for descriptions of method abbreviations used in the Method column. **Numsamples:** Total number of samples. **NumLCC:** Number of samples with left-censored concentrations. **minLCT:** Lowest left-censored threshold. **modeLCT:** Mode of the left-censored threshold. **maxLCT:** Highest left-censored threshold. **NumNCC:** Number of non-censored concentrations. **minNCC:** Minimum non-censored concentration. **modeNCC:** Mode of the non-censored concentrations. **maxNCC:** Maximum of the non-censored concentrations. **Abbreviation and symbols:** nd, not determined;<, less than; >, greater than]

Method	Numsamples	NumLCC	minLCT	modeLCT	maxLCT	NumNCC	minNCC	modeNCC	maxNCC
Ba summary									
AES_AR_P	9,923	94	<0.02	<0.2	<0.2	9,829	0.025	110	1,800
MS_AR_P	693	0	nd	nd	nd	693	40	180	627
Cr summary									
method	Numsamples	NumLCC	minLCT	modeLCT	maxLCT	NCC	minNCC	modeNCC	maxNCC
AES_AR_P	12,265	2,505	<0.015	<1.2	<63	9,760	1.2	22	794
MS_AR_P	693	0	nd	nd	nd	693	5	28	207
AES_Acid_P	61	0	nd	nd	nd	61	12	34	52
Co summary									
AES_AR_P	12,528	2,088	<1	<1	<63	10,440	0.79	11	410
AA_F_AR_P	300	3	<1	<1	<1	297	1	16	237
AA_F_HNO3_P	139	50	<10	<10	<10	89	6	10	120
MS_AR_P	693	0	nd	nd	nd	693	2.1	12.5	44.4
AA_F_DTPA_P	2	2	<0.5	<0.5	<0.5	0	nd	nd	nd
AES_Acid_P	61	0	nd	nd	nd	61	5	9	21
Cu summary									
AES_AR_P	12,255	124	<0.15	<0.2	<12	12,131	0.19	15	7,000
AA_F_AR_P	4,156	2	<0.5	<0.5	<0.5	4,154	1	20	1,150
CM_Fuse_P	770	17	<2	<2	<2	753	2	40	17,000
CM_Acid_P	1,521	9	<5	<5	<5	1,512	5	20	500
AA_F_HNO3_P	25,849	569	<1	<5	<20	25,280	0.12	20	15,000
AES_AZ_P	8,811	3	<0.05	<0.05	<0.75	8,808	0.3	12	5,000

48

Method	Numsamples	NumLCC	minLCT	modeLCT	maxLCT	NumNCC	minNCC	modeNCC	maxNCC
Cu summary (continued)									
MS_AR_P	693	0	nd	nd	nd	693	2.1	16.5	111
AA_F_AZ_H2O2_P	213	27	<5	<5	<5	186	5	40	820
AA_F_AZ_Fuse_P	37	0	nd	nd	nd	37	15	25	260
AA_F_DTPA_P	2	0	nd	nd	nd	2	2	2	6
AES_Acid_P	61	0	nd	nd	nd	61	11	15	48
Ni summary									
AES_AR_P	8,911	390	<1	<1	<15	8,521	1.1	22	1,550
CM_Acid_P	532	4	<5	<5	<5	528	5	40	1,500
AA_F_Acid_P	68	0	nd	nd	nd	68	25	75	120
AA_F_HNO3_P	329	2	<5	<5	<5	327	6	40	800
MS_AR_P	692	0	nd	nd	nd	692	5	36	852
AA_F_DTPA_P	2	1	<1	<1	<1	1	1	1	1
AES_Acid_P	61	0	nd	nd	nd	61	12	16	30
Pb summary									
AA_F_AR_P	5,891	72	<1	<1	<1	5,819	2	10	940
AES_AR_P	9,968	5,300	<2	<3.5	<63	4,668	1	12	740
CM_HNO3_P	76	0	nd	nd	nd	76	5	5	215
CM_Fuse_P	775	56	<4	<4	<4	719	4	10	715
CM_Acid_P	1,968	11	<5	<5	<5	1,957	5	10	2,900
AA_F_HNO3_P	24,204	1,906	<0.25	<25	<258	22,298	0.5	10	>100,000
AES_AZ_P	8,811	158	<0.6	<0.67	<75	8,653	0.6	11	3,400
MS_AR_P	692	2	<2	<2	<2	690	3	7	335
AA_F_AZ_H2O2_P	173	26	<5	<5	<5	147	5	10	70
AA_F_AZ_Fuse_P	42	0	nd	nd	nd	42	5	10	35
AA_F_DTPA_P	2	1	<1	<1	<1	1	4	4	4
AES_Acid_P	61	4	<2	<2	<2	57	2	12	108

Method	Numsamples	NumLCC	minLCT	modeLCT	maxLCT	NumNCC	minNCC	modeNCC	maxNCC
				Zn summary					
AES_AR_P	12,141	219	<0.15	<0.3	<1	11,922	0.34	63	31,000
AA_F_AR_P	3,692	5	<1	<1	<1	3,687	3	60	19,400
CM_HNO3_P	277	68	<25	<50	<1,400	209	30	50	1,400
CM_Fuse_P	772	45	<5	<5	<5	727	5	60	2,500
CM_Acid_P	1,517	6	<5	<5	<5	1,511	10	80	13,000
AA_F_Acid_P	474	0	nd	nd	nd	474	40	90	410
AA_F_HNO3_P	37,057	71	<5	<25	<25	36,986	5	60	45,000
AES_AZ_P	9,417	3	<0.03	<1	<1	9,414	2.7	110	6,000
AA_F_AZ_H2O2_P	4,578	21	<5	<5	<5	4,557	5	60	30,000
MS_AR_P	693	0	nd	nd	nd	693	6	78	207
AA_F_AZ_Fuse_P	3,433	9	<5	<5	<5	3,424	5	100	25,000
AA_F_AZ_HCl_P	43	0	nd	nd	nd	43	20	90	260
AA_F_DTPA_P	2	0	nd	nd	nd	2	1	1	1
AES_Acid_P	61	0	nd	nd	nd	61	43	88	216

Table 4. Number of Alaskan samples analyzed, left-censored data characteristics, and non-censored data characteristics for the semiquantitative visual six-step direct-current arc emission spectrographic method (ES_SQ) used to determine barium (Ba), chromium (Cr), cobalt (Co), copper (Cu), nickel (Ni), lead (Pb), and zinc (Zn) concentrations.

[**Numsamples:** Total number of samples. **NumLCC:** Number of samples with left-censored concentrations. **minLCT:** Lowest left-censored threshold. **modeLCT:** Mode of the left-censored threshold. **maxLCT:** Highest left-censored threshold. **NumNCC:** Number of non-censored concentrations. **minNCC:** Minimum non-censored concentration. **modeNCC:** Mode of the non-censored concentrations. **maxNCC:** Maximum of the non-censored concentrations. **Symbols:** <, less than; >, greater than]

Element	Numsamples	NumLCC	minLCT	modeLCT	maxLCT	NumNCC	minNCC	modeNCC	maxNCC
Barium	73,686	313	<2	<20	<100	73,373	3	700	>100,000
Chromium	75,752	1,217	<1	<10	<20	74,535	1.5	100	10,000
Cobalt	75,817	2,745	<2	<5	<10	73,072	1.06	20	1,000
Copper	75,821	1,338	<1	<5	<10	74,483	1.23	30	50,000
Nickel	75,801	1,444	<1	<5	<10	74,357	2	50	>5,000
Lead	75,812	11,237	<5	<10	<10	64,575	1	20	50,000
Zinc	74,981	66,328	<20	<200	<10	8,653	15	200	>100,000

Table 5. Method combinations involving two analytical methods with total decomposition of the Alaskan samples.

[See section, "Method Abbreviations" for descriptions of method abbreviations used in the Methods columns. Blank cells indicate that the combination is not present in the database for that element. **ntot:** Total number of samples. **n*:** Number of sample pairs with concentrations that have detected concentrations by both methods]

Methods		Barium (Ba)		Chromium (Cr)		Cobalt (Co)		Copper (Cu)		Nickel (Ni)		Lead (Pb)		Zinc (Zn)	
Method 1	Method 2	ntot	n*	ntot	n*	ntot	n*	ntot	n*	ntot	n*	ntot	n*	ntot	n*
AES_Fuse	WDX_Fuse			20	11										
AES_HF	NA[1]	5,890	5,374	5,878	5,608	5,866	5,561			935	506			5,819	2,298
AES_HF	EDX							4,909	4,627	4,910	3,926	4,907	2,802		
AES_HF	AES_ST	765	765	765	760			773	724	773	765			773	773
AES_HF	MS_Fuse	684	684	684	684	32	32								
AES_HF	AES_Fuse	22	22	22	22										
AES_HF	MS_HF	6	6	6	6	97	97	6	6	6	6	97	97	6	6
AES_HF	WDX_Fuse			44	11										
AES_HF	MS_ST					315	314					323	223		
AES_ST	NA	7	7	7	7									8	2
AES_ST	WDX_Fuse			44	26										
EDX	AES_ST							8	8	8	8				
EDX	NA									4	4				
EDX	MS_HF											3	1		
EDX	MS_ST											8	3		
MS_Fuse	AES_HF_UT	50	50	50	50										
MS_HF	MS_ST					450	450					450	441		
MS_HF	NA							3	3						
NA	MS_ST					7	7								

[1]Includes National Uranium Resource Evaluation (NURE) and non-NURE analysis.

Table 6. Method combinations involving two analytical methods one with a total decomposition of the sample and the other with a partial decomposition of the Alaskan samples.

[See section, "Method Abbreviations" for descriptions of method abbreviations used in the Methods columns. Blank cells indicate that the combination is not present in the database for that element. **ntot:** Total number of samples. **n*:** Number of sample pairs with concentrations that have detected concentrations by both methods]

Methods		Barium (Ba)		Chromium (Cr)		Cobalt (Co)		Copper (Cu)		Nickel (Ni)		Lead (Pb)		Zinc (Zn)	
Method 1	Method 2	ntot	n*	ntot	n*	ntot	n*	ntot	n*	ntot	n*	ntot	n*	ntot	n*
AES_HF	AES_AR_P	281	278	1,162	1,082	280	270	1,069	1,060	1,182	1,155	280	59	1,069	1,056
AES_HF	MS_AR_P	1	1	1	1	1	1	1	1						
AES_HF	AA_F_AR_P							1,030	1,015			918	907	1,029	1,029
AES_HF	AA_F_HNO3_P							1,005	976			930	902	1,280	1,280
AES_HF	AES_AZ_P							3,726	3,720			2,852	2,587	3,819	3,818
AES_HF	AA_F_AZ_H2O2_P							10	10			9	9	73	73
AES_HF	MS_AR_P													1	1
AES_HF	AA_F_AZ_Fuse_P													8	8
AES_ST	AES_AR_P	64	64	28	24			28	27	28	25			28	28
AES_ST	AA_F_HNO3_P							1,202	1,181	107	107			2,345	2,344
AES_ST	AES_AZ_P							603	574					603	603
AES_ST	AA_F_AZ_H2O2_P							4	4					173	172
AES_ST	CM_HNO3_P													48	48
AES_ST	AA_F_AZ_Fuse_P													597	597
EDX	AES_AR_P							452	447	452	279	452	168		
EDX	AES_AZ_P							282	272			282	120		
EDX	MS_AR_P							77	77	77	75	76	74		
MS_HF	AES_AR_P					903	549					1	1		
MS_HF	AA_F_AR_P											901	901		
MS_HF	AA_F_HNO3_P											47	47		
MS_HF	AES_AZ_P											971	968		
MS_ST	AES_AR_P					28	22					28	3		
MS_ST	AA_F_HNO3_P											951	829		
MS_ST	AES_AZ_P											603	580		

53

Methods		Barium (Ba)		Chromium (Cr)		Cobalt (Co)		Copper (Cu)		Nickel (Ni)		Lead (Pb)		Zinc (Zn)	
Method 1	Method 2	ntot	n*	ntot	n*	ntot	n*	ntot	n*	ntot	n*	ntot	n*	ntot	n*
MS_ST	AA_F_AZ_H2O2_P											4	4		
NA	AES_AR_P	1,557	1,500	1,557	1,523	1,557	1,500			1,103	504			1,557	261
NA	MS_AR_P	77	75	77	76	77	77							77	8
NA	AA_F_AR_P													914	34
NA	AES_AZ_P													282	116

Table 7. Method combinations involving semiquantitative visual six-step direct-current arc emission spectrography and an analytical method with total decomposition of the Alaskan samples.

[See section, "Method Abbreviations" for descriptions of method abbreviations used in the Methods columns. Blank cells indicate that the combination is not present in the database for that element. **ntot:** Total number of samples. **n*:** Number of sample pairs with concentrations that have detected concentrations by both methods]

Methods		Barium (Ba)		Chromium (Cr)		Cobalt (Co)		Copper (Cu)		Nickel (Ni)		Lead (Pb)		Zinc (Zn)	
Method_1	Method_2	ntot	n*	ntot	n*	ntot	n*	ntot	n*	ntot	n*	ntot	n*	ntot	n*
AES_HF	ES_SQ	2,535	2,528	2,589	2,555	2,425	2,394	2,597	2,578	2,597	2,540	2,433	1,987	2,596	344
NA	ES_SQ	1,511	1,416	1,511	1,457	1,511	1,405							1,510	48
AES_ST	ES_SQ	4,849	4,814	4,997	4,819			5,005	4,874	4,999	4,828			5,005	470
MS_ST	ES_SQ					4,997	4,903					5,005	4,329		
MS_HF	ES_SQ					245	220					245	231		
EDX	ES_SQ							1,451	1,425	1,451	1,375	1,451	1,098		
AA_F_HF	ES_SQ					21	21					21	0	298	279

Appendix 1. Common Methods in the Compiled Dataset

Instrumental neutron activation analysis (NA), energy-dispersive x-ray spectrometry (EDX), and semiquantitative visual six-step direct-current arc emission spectrography (ES_SQ) are the most common methods for many elements with concentration data in the Alaska Geochemical Database (AGDB). NA and EDX were the primary methods used for the Alaska samples collected during the National Uranium Resource Evaluation (NURE) program (Information Systems Programs Energy Resources Institute, 1985). ES_SQ was commonly used in the U.S. Geological Survey (USGS) programs from the 1960s through the 1980s (Myers and others, 1961; Grimes and Marranzino, 1968; Motooka and Grimes, 1976). Because of their prevalence in the dataset, these methods are summarized individually.

Instrumental Neutron Activation Analysis and Delayed Neutron Counting

NA and delayed neutron counting (DN) use neutron irradiation of a sample to transform stable isotopes of an element into radioactive isotopes. The abundance of the element in the sample is determined by measuring the radiation from the decay of the induced indicator radionuclide (Baedecker and McKown, 1987; McKown and Millard, 1987; Potts, 1992). The basis of the NA analysis is the emission of characteristic beta and gamma radiation by decay of indicator radionuclides (Baedecker and McKown, 1987; McKown and Millard, 1987, Potts, 1992). The time between sample irradiation and gamma-ray counting is varied to optimize detection of both short- and long-lived indicator radionuclides. The detection limits for NA depend on sample composition, particularly the sodium (Na), scandium (Sc), iron (Fe), cobalt (Co), and lanthanum (La) concentrations in the sample because decay activation products of these elements dominate the spectrum and limit the sensitivity for determining other elements for several days following irradiation (Baedecker and McKown, 1987). Factors affecting the precision of NA include:

- Non-uniform neutron flux across the sample during irradiation,
- Non-reproducible sample positioning during counting, and
- Poor counting statistics and photopeak baseline selection.

Factors affecting accuracy include:

- Interfering nuclear reactions from elements that yield the same indicator radionuclide as the element of interest, which is a concern for cerium determination when uranium is present;
- Gamma-ray spectral interferences, which is a concern for both zinc and barium determination;
- Self-shielding, which is of limited concern in most silicate matrices but of concern in the analysis of rare earth element minerals;
- Dead-time errors;
- Powder density differences; and
- Errors in the preparation or calibration of the standards (Baedecker and McKown, 1987; Potts, 1992).

DN analysis is used in determining the concentrations of heavy nuclei, such as thorium, uranium, and the transuranium elements. When irradiated, these elements produce an

55

energetically unstable nucleus that fissions into two lighter-element nuclei and releases one or more neutrons (known as prompt neutrons). Most fission products decay by a series of beta emissions. However, some fission products decay by beta emissions accompanied by the release of a neutron (a delayed neutron). The delayed neutrons are detected and counted quantitatively (McKown and Millard, 1987).

The NURE program in Alaska included determinations of the concentrations of 31 elements by NA and uranium by DN. Sample size usually was about 5 g, but as little as 0.5 g was sometimes used (Bolivar, 1987). Instrumental details and settings, briefly summarized here, are given in Minor and others (1982) and Information Systems Programs Energy Resources Institute (1985). Samples were transferred to 4 mL irradiation vials (known as rabbits) made of high-purity, ethylene-butylene copolymer and loaded into an automatic sampler that transferred the sample along the automated analytic sequence (Minor and others, 1982). Each sample was analyzed using the following timing sequence designed to facilitate sample throughput: 20-second irradiation, 10-second delay, 30-second DN analysis for uranium, 20-minute delay, 500-gamma-ray count for short-lived radionuclides by NA, irradiation for 96 seconds, a 14-day delay, and then a 1,000-second gamma-ray count for long-lived radionuclides by NA (Minor and others, 1982; Information Systems Programs Energy Resources Institute, 1985). Sample concentrations were considered below detection when the statistical counting error exceeded 50 percent (Information Systems Programs Energy Resources Institute, 1985). The detection limits reported for each element determined by NA are a function of the total composition and mass of the individual sample. However, statistical detection-limit determinations on a typical 4-g stream sediment sample run at maximum throughput were determined by Minor and others (1982) (appendix 1, table 1.1). The uncertainty in the trace element concentrations measurements for NA were given by the NURE program as less than 10 percent at concentrations 1 order of magnitude greater than the statistical detection limit (Minor and others, 1982; Information Systems Programs Energy Resources Institute, 1985).

Energy Dispersive X-Ray Fluorescence Spectrometry

EDX is a spectrographic technique that can be used either as a qualitative or quantitative elemental analytical tool for solid and liquid samples. During analysis, a high-energy source irradiates samples and the x-ray fluorescence generated by the sample is measured. Normally, an x-ray tube is the energy source but radioactive sources, such as ^{55}Fe or ^{109}Cd, can be used. A typical x-ray tube is composed of a solid target that can be made of many metals and a filament, usually made of tungsten. The x-rays used for irradiation are energetic enough to eject an electron from an atom's inner shell, leaving the atom in an unstable excited state. When the atom's electronic configuration returns to its stable ground state, element-specific x-ray photons (fluorescence) are emitted and detected using lithium-drifted silicon detectors that convert the incident x-rays into electronic pulses. The peak intensity corresponds to the number of fluorescing atoms of an element in the sample; the area under a peak is proportional to the concentration of that element in the sample (Johnson and King, 1987; Taggart and others, 1987).

To obtain good intensity to concentration characteristics, samples must be prepared so that the surface is smooth and flat, and the particle size is uniform. Loose powders, briquettes, and fused disks are sample preparations used in EDX analysis. Loose powder preparations are quick but are subject to variable packing densities and are not free of particle size or mineralogical effect. Briquette formation helps to reduce effects of packing density but are time consuming and do not eliminate completely particle size or mineralogical effects. Fused disks

eliminate particle size or mineralogical effects but some materials, such as coal, do not fuse and others, such as sulfides, volatilize on fusion (Johnson and King, 1987). The precision depends primarily on instrument stability, although it also can be influenced by variations in specimen preparation or by differences in sample geometry within the spectrometer. Accuracy is affected by numerous factors including non-uniform sample preparation, atomic number of the elements (matrix affects lighter elements more than heavier elements), and line interferences. The detection limits depend on atomic numbers, background, spectral overlaps, excitation sources, and sample preparation methods (Johnson and King, 1987).

Concentrations of Ag, Bi, Cd, Cu, Nb, Ni, Pb, Sn, and W in sediment samples were determined by EDX during the NURE program in Alaska. Analysis was performed on loose powder preparations. Six grams of the 100-mesh sediment sample were ground to a minus 325-mesh powder and transferred to a 3.2-cm polypropylene sample cell and covered with 0.006 mm-thick Mylar. The powder was compacted against the Mylar by inverting the cell and tapping it on a smooth surface. The grinding containers were found to have low Ni and Cu content, and only a little Fe was added owing to grinding. The EDX system consisted of an automatic 20-position sample charger, a silicon lithium-drift detector, a pulsed molybdenum transmission-target x-ray tube, and a multi-channel analyzer. Operating conditions were as follows:

- Excitation potential, 50 kilovolts;
- Current, 0.15 milliamperes;
- Filter between x-ray tube and sample, 0.177 mm molybdenum;
- Live counting time, 350 seconds; and
- Energy range (iron K-alpha emission lines in x-ray spectroscopy [Kα] to tin Kα) 6-26 kiloelectron volts.

Sample positioning in the x-ray beam, overlapping peaks deconvolution, peak intensity determination, and the calculation of the individual peak intensities compared to that of the molybdenum Kα Compton peak were computer controlled. Elemental concentrations were determined using equations derived from the analysis of prepared standards. The precision, reported as the relative standard deviation, was determined on blanks spiked with either 20 or 100 parts per million (ppm) of each element. Precision was plus or minus (±) 10 percent or less at the 100-ppm level and ±20 percent or less at the 20-ppm level. The detection limits used were defined as 3 times the standard deviation of 10 measurements of a blank and are given in appendix 1, table 1.1. The high Nb detection limit results from molybdenum Compton interference (Hansel and Martell, 1977).

Semiquantitative Direct-Current Arc Emission Spectrography

Direct-current (DC) arc emission spectrography is an optical emission technique. Atomization or ionization and excitation of the sample are achieved by an electrical discharge between two electrodes. One electrode is composed of the sample, typically mixed with high-purity graphite, and the other typically is high-purity graphite. The electrodes are separated by a small gap. Electrical heating of the electrodes vaporizes, ionizes, and atomizes material from the electrode tips into the gap. The atomic and ionic species present are excited to a higher electrical state in an electrical plasma discharge generated within the gap. The intensity of selected emission lines generated as the excited atomic and ionic species return to their ground state is detected by optical spectrographs or spectrometers. Precision and accuracy of this technique are negatively affected by lack of control of the gap distance during the arcing process and transport

and dissociation of materials into the gap. In geological samples, the technique is subject to matrix effects that include the sample's particle size, mineralogical characteristics, and the possible formation of non-volatile carbides. The technique most frequently was used for semiquantitative analysis (Golightly and others, 1987; Potts, 1992).

The concentrations of 30 elements (appendix 1, table 1.1) were determined by DC arc emission spectrography as part of numerous USGS projects and programs from the 1950s to the early 1990s. The method most frequently used was a semiquantitative visual six-step method that subdivided each order of magnitude of concentration interval into six steps. The steps were the approximate geometric midpoints of the concentration ranges whose boundaries are given in table 1 of the report. Analytical results were rounded and reported to the nearest step. Samples were prepared for analysis by mixing 10 g of sample with 20 g of graphite or a graphite-quartz mixture. The mixture was packed into a preformed graphite electrode and volatilized in a DC arc that results in nearly complete decomposition of the sample (Grimes and Marranzino, 1968). Synthetic standards were prepared by adding compounds, usually the oxide or carbonate, of the elements of interest to a simple synthetic rock matrix (matrix contained about 33 percent Si, 7 percent Fe, 3.7 percent Al, 2 percent Ca, 1.6 percent Na, 1.1 percent K, and 0.6 percent Mg). Three standards were prepared per order of magnitude. Intermediate steps were visually interpolated. The reported limit of determination is given in appendix 1, table 1.1 (Grimes and Marranzino, 1968; Motooka and Grimes, 1976).

Other Methods

Most of the other methods used to generate the concentration data in the compiled dataset require chemical decomposition prior to instrumental analysis. Acid dissolution and flux decomposition, either by fusion or sintering, commonly were used to decompose the samples. Acid dissolution and flux decomposition can be considered total or partial decomposition techniques depending on the particular decomposition protocol (Chao, 1984; Chao and Sanzolone, 1992). Decomposition techniques using hydrofluoric acid (HF) are considered a total dissolution technique and those without HF, including the commonly used 1:3 volume ratio mixture of nitric acid (HNO_3) and hydrochloric acid (HCL), acids known as "aqua regia," are considered a partial technique. Most of the flux decompositions used to prepare the sample for multi-element analysis are considered total decomposition. Although various decomposition techniques are considered total or partial techniques, the true extent of decomposition of a sample will depend on the mineralogical composition of that sample. Important characteristics for acid dissolutions include the oxidizing power of an acid and its efficacy in breaking the silicon-to-oxygen bond in silicate minerals. Whether a flux is it is alkali or acid and oxidizing or reducing in a reaction are important characteristics (appendix 1, tables1.2 and 1.3; Chao and Sanzolone, 1992). Other considerations are as follows:

- Possible loss of elements due to formation of volatile compounds (for example, fluorides of As, B, Ti, Nb, Ta, Ge, Sb, and Si during dissolution with HF);
- Formation of insoluble compounds;
- Availability of high purity acids or fluxes; and
- For fluxes, the flux composition relative to the elements of interest (Na and Li cannot be determined in a sample decomposed with fluxes containing Na and Li, respectively) (Chao and Sanzolone, 1992).

Following chemical decomposition, various analytical instruments can be used to quantify the elements of interest. Inductively coupled plasma-atomic emission spectrometry (ICP-AES), inductively coupled plasma-mass spectrometry (ICP-MS), and atomic absorption (AA) spectrometry are common instrumental techniques used for the quantification of elements. For example, elemental analysis by ICP-MS following sample decomposition by a sinter technique (ST) (AGDB method abbreviation MS_ST). Both ICP-AES and ICP-MS are multi-element techniques capable of high throughput with good sensitivity for many elements and are the principal analytical instruments used, either separately or together, to analyze the digestion of geologic samples. AA still has considerable use in the detection of specific elements, particularly arsenic, mercury, antimony, and the noble metals.

Table 1.1. Detection limits for the most commonly occurring methods in the combined dataset.

[See section "Method Abbreviations" for descriptions of method abbreviations used in table headings. See section "List of Chemical Symbol" for element symbols and element name used in table. **Wavelength (Å):** Grimes and Marrazino (1968). Blank cells indicate that the element was not analyzed by the method in the column. Wavelengths in parentheses are alternate wavelengths used. **Lower detection limits for elements analyzed by EDX during the NURE program:** Hansel and Martell (1977); Information Systems Programs Energy Resources Institute (1985). Lower detection limits for EDX analysis performed by NURE were defined as 3 times the standard deviation of 10 measurements of the blank. Precision was determined on blanks spiked with either 20 or 100 ppm of each element. Relative standard deviation (RSD) varies by element. RSDs determined at 100 ppm were: Ni, 8 percent (%); Cu, 8%; W, 10%; Pb, 4%; Bi,3%; Nb, 7%; Ag, 2%; Cd, 2%; and Sn, 4%. The RSDa determined at 20 ppm were: Ni, 38%; Cu, 27%; W, 25%; Pb, 10%; Bi, 9%; Nb, 27%; Ag, 9%; Cd, 8%, and Sn, 14%. **Lower detection limits for elements analyzed by NA and DN during the NURE program:** Minor and others (1982); Information Systems Programs Energy Resources Institute (1985). Detection limits by NA are a function of sample composition and mass used. Lower detection limits for INAA analysis performed by the NURE program were average values calculated from a typical 4-gram sample. Values are presented in the Information Systems Programs Energy Resources Institute report. Values in parentheses are from Minor and others (1982). Uncertainties (relative error) in the measured trace element concentrations for NA under the NURE program in Alaska usually are less than 10% at concentrations an order of magnitude higher than the lower detection limit. **Reporting limits for ICP-AES—Compiled dataset acronym AES_HF:** Briggs (2002). Lower detection limits were defined as 3 times the standard deviation determined from the method blank or low analyte concentration samples are given in parentheses for the elements also analyzed by EDX in NURE samples (Taggart, 2002). Parenthetical values are more analogous to the lower detection limits given for the NURE EDX determinations (Hansel and Martell, 1977). **Lower limit of determination for ICP-MS—Compiled dataset acronym MS_HF:** Briggs and Meier (2002). Lower limit of determination is taken 5 times the standard deviation determined from the method blank or low analyte concentration samples (Taggart, 2002). **Abbreviations:** NURE, National Uranium Resource Evaluation; Å, angstroms; nm, nanometers; ppm, parts per million]

Element	Wavelength and lower limit of determination for ES_SQ.		Lower detection limits for elements analyzed by EDX during the NURE program (ppm)	Lower detection limits for elements analyzed by NA and DN during the NURE program (ppm)	Reporting limits for ICP-AES—Compiled dataset acronym AES_HF		Lower limit of determination for ICP-MS—Compiled dataset acronym MS_HF	
	Wavelength (Å)	Lower limit of determination (ppm)			wavelength (nm)	ppm	Mass	ppm
Ag	3,280.7 (3,382.9)	0.5	5		328.0	2 (0.3)	108.905	0.0036
Al				3,200	308.2	50 (4)	26.982	53.0000
As	2,860.4 (2,780.2)	200	5		188.9	10 (2)	74.922	0.1800
Au	2,675.9	10		0.05	242.7	8 (2)	196.967	0.0033
B	2,497.7	10						
Ba	4,554.0 (2,335.3)	5		150	413.1	1 (0.03)	137.905	0.2600
Be	3,131.1	1	1		313.0	1 (0.02)	9.012	0.0290
Bi	3,067.7	10	5		223.0	1 (3)	208.98	0.0560

Element	Wavelength and lower limit of determination for ES_SQ.		Lower detection limits for elements analyzed by EDX during the NURE program (ppm)	Lower detection limits for elements analyzed by NA and DN during the NURE program (ppm)	Reporting limits for ICP-AES—Compiled dataset acronym AES_HF		Lower limit of determination for ICP-MS—Compiled dataset acronym MS_HF	
	Wavelength (Å)	Lower limit of determination (ppm)			wavelength (nm)	ppm	Mass	ppm
Ca	3,158.8	500		1,000	430.2	50 (7)	42.959	130.0000
Cd	3,261.1	20	5		226.5	2 (0.2)	113.904	0.0069
Ce				10	413.7	5 (2)	139.905	0.0900
Cl				50				
Co	3,453.5	5		1.7	228.6	2 (0.5)	58.933	0.0250
Cr	4,254.3	5		10	267.7	2 (0.3)	51.941	0.4800
Cs				2 (10)				
Cu	3,273.9	2	10		324.7	2 (0.8)	64.928	1.4000
Dy				0.7				
Er								
Eu				0.4	381.9	2 (0.06)	150.92	0.0015
Fe	3,100.6	500		1,100	273.9	200 (60)	56.935	45.0000
Ga					294.3	4 (1)	70.925	0.0130
Gd								
Ge								
Hf				1.3				
Hg								
Ho					345.6	4 (0.2)	164.93	0.0010
In								
Ir								
K				3,400	766.4	100 (5)	38.964	15.0000
La	3,337.5	20		7	408.6	2 (0.4)	138.906	0.0480
Li			1		670.7	2 (0.03)	7.016	0.3100
Lu				0.1				
Mg	2,781.4	200		2,700	279.0	50 (2)	24.986	5.8000

Element	Wavelength and lower limit of determination for ES_SQ.		Lower detection limits for elements analyzed by EDX during the NURE program (ppm)	Lower detection limits for elements analyzed by NA and DN during the NURE program (ppm)	Reporting limits for ICP-AES—Compiled dataset acronym AES_HF		Lower limit of determination for ICP-MS—Compiled dataset acronym MS_HF	
	Wavelength (Å)	Lower limit of determination (ppm)			wavelength (nm)	ppm	Mass	ppm
Mn	2,949.2	10		55	257.6	4 (0.2)	54.938	0.7100
Mo	3,170.3 (3,193.9)	5			202.0	2 (0.7)	97.906	0.0530
Na				1,000	589.5	60 (20)	22.99	27.0000
Nb	3,163.4	10	20		292.7	4 (0.3)	92.906	0.1100
Nd					406.1	4 (3)	145.913	0.0250
Ni	National Uranium Resource Evaluation	2	15		231.6	3 (0.9)	59.933	0.2600
Os								
P					213.6	50 (5)	30.994	5.1500
Pb	2,833	10	5	5	220.3	4 (1)	207.977	0.3700
Pd								
Pr								
Pt								
Rb								
Re								
Rh								
Ru				13				
Sb	2,877.9	100		1			120.904	0.0430
Sc	3,353.7	5		0.9	424.6	2 (0.2)	44.956	0.0340
Se			5					
Si								
Sm				0.4				
Sn	3,175.0 (2,839.9)	10	10		189.9	5 (0.4)	117.902	0.1200
Sr	4,607.3 (3,464.4)	50		400 (110)	460.7	2 (0.04)	87.906	0.8300
Ta				1	240.0	40 (2)	180.948	0.0120
Tb				1				

Element	Wavelength and lower limit of determination for ES_SQ.		Lower detection limits for elements analyzed by EDX during the NURE program (ppm)	Lower detection limits for elements analyzed by NA and DN during the NURE program (ppm)	Reporting limits for ICP-AES—Compiled dataset acronym AES_HF		Lower limit of determination for ICP-MS—Compiled dataset acronym MS_HF	
	Wavelength (Å)	Lower limit of determination (ppm)			wavelength (nm)	ppm	Mass	ppm
Te								
Th				1	350.9	4 (2)	232.038	0.0950
Ti	3,168.5	10		750	223.0	50 (0.9)	49	4.1000
Tl							204.975	0.0790
Tm								
U				0.01*	385.9	100 (6)	238.05	0.0230
V	3,102.3 (3,183.9)	10		6	292.4	2 (0.4)	50.944	0.1400
W	2,946.9	50	15					
Y	3,327.8	10		1	371.0	2 (0.3)	88.905	0.0470
Yb					328.9	1 (0.4)	171.937	0.0061
Zn	3,345.0 (3,302.6)	200		100 (11)	213.8	2(0.2)	65.926	2.3000
Zr	3,279.2	20	5					

Table 1.2. Characteristics of acids decomposition techniques (Chao and Sanzolone,1992).

[See section, "List of Chemical Element Symbols" for element symbols and element names used in table]

Acid	Oxidizing	Non-oxidizing	Characteristics
Hydrofluoric acid (HF)		x	HF is effective at breaking the silicon oxygen bond (SiO)bond and forms silicon tetrafluoride (SiF_4), which volatilizes upon heating. Metals bound within the silicate structure are released as the Si lattices are destroyed. Any As, B, Ti, Nb, Ta, Ge, and Sb present in the sample's mineral will be totally or partially lost through formation and volatilization of their respective fluorides. Some elements form insoluble fluoride compounds (for example, barium fluoride (BaF_2) and lead fluoride (PbF_2)) or will coprecipitate with insoluble fluorides (for example, Rb, Sr, Y, Cs, Ba, rare earth elements (REE), Pb, Th, and U) (Yokoyama and others, 1999). HF typically is used in conjunction with other mineral acids such as $HClO_4$, HNO_3, HCl, aqua regia (see definition below in Nitric acid discussion, or H_2SO_4) that facilitate the decomposition of the non-silicate rock minerals (for example, sulfides and oxides).
Hydrochloric acid (HCl)		x (reducing)	Dissolves carbonates, phosphates, borates, and sulfates except barite. Solubilizes acid-volatile sulfides (AVS) that consist of poorly crystallized secondary sulfides and monosulfides but has limited effect on pyrite. The dissolution of sulfide minerals is increased considerably when HCl is combined with an oxidant such as potassium chlorate ($KClO_3$) or peroxide (H_2O_2). HCl is more effective than HNO_3 at dissolving iron and manganese oxides because it can be a reducing agent in redox reactions, and it can produce chloride complexes. HCl usually is mixed with other acids, especially HNO_3, in dissolution schemes for silicate minerals. HCl often is used to dissolve the melts of alkali fusion decomposition or the residual materials of other acid digestions.
Hydrobromic acid (HBr)		x	HBr is less commonly used than HCl for sample decomposition. HBr photolyses when exposed to light and releases free bromine. Inclusion of an oxidant such as sodium bromate ($NaBrO_3$) or concentrated HNO_3 enhances sample decomposition. In such combinations, the free bromine, liberated by the oxidant, reacts with sulfides, sulfoarsinides, and arsenides, making them more soluble in the acid. Br- is a strong ligand for complexing metals including Au.
Nitric acid (HNO_3)	x		Hot, concentrated HNO_3 is a strong oxidizing acid. It decomposes sulfides, selenides, tellurides, arsenides, and sulfoarsenides through oxidative degradation and readily dissolves carbonates but is less effective than HCl in dissolving iron and manganese oxides. HNO_3 is commonly used to digest soil and sediments in geochemical exploration work but extraction is not always total. Aqua regia is a commonly used mixture of HNO_3 and HCl in a 1:3 volume ratio. This mixture has a much stronger oxidizing and dissolving power than HNO_3 alone. Aqua regia is used in numerous decomposition schemes either alone or with HF. Aqua regia attacks Au, Pt, and Pd and decomposes sulfides including pryrite, arsenides, selenides, and some Mo and W minerals. The strength of aqua regia is enhanced by adding free bromide. The aqua regia-Br_2 mixture has been used as a dissolution regime for Ag, Au, Cd, Se, Te, and Tl determinations.

Acid	Oxidizing	Non-oxidizing	Characteristics
Perchloric acid ($HClO_4$)	x		Hot, concentrated $HClO_4$ is a powerful oxidizing and dehydrating acid capable of decomposing sulfides and organic matter. Its oxidizing power is diminished by dilution with water. $HClO_4$ has a high boiling point and is used to drive off HF and other more volatile acids by fuming. Perchlorates of K, Rb, and Cs are not water soluble, but all others are water soluble. $HClO_4$ is most frequently used with other acids, particularly HF, in decomposition schemes.
Sulfuric acid, (H_2SO_4)	x		Concentrated H_2SO_4, alone or in combination with other acids, is not widely used in the decomposition of geological samples. This is because of the low solubility of alkaline earth and lead sulfates, and the interference of the sulfate with the alkaline earth metals conducting atomic absorption spectrometry analysis. H_2SO_4 is an oxidizing acid, but its oxidizing power is diminished by dilution with water. Hot concentrated H_2SO_4 can decompose monazite; sulfides of As, Sb, Se, and Te, and Nb; and Ta minerals in the presence of ammonium sulfate ($(NH_4)_2SO_4$). Naturally occurring fluoride minerals can be decomposed by evaporation with H_2SO_4.
Orthophophoric acid (H_3PO_4)		x	H_3PO_4 is not frequently used for silicate analysis because of complexing or precipitating of some elements. However, it effectively decomposes chromite; when combined with HF, HNO_3, and (or) $HClO_4$ or H_2O_2, H_3PO_4 can decompose sulfides for Cu, silicate rocks and sulfides for Ge, soils for Se, and geochemical samples for Au determinations.

Table 1.3. Characteristics of flux decomposition techniques (Chao and Sanzolone, 1992).

[See section "List of Chemical Element Symbols" for element symbols and element names used in table]

Flux	Alkali	Acid	Oxidizing	Characteristics
Sodium carbonate (Na_2CO_3) and sodium hydroxide (NaOH)	x		Yes	Na_2CO_3 and NaOH fluxes were used extensively to convert sample elements into soluble silicates and aluminates or to precipitates, which are more easily dissolved by acid than the original mineral forms. To improve the decomposition of sulfides, arsenides, and other reducing materials, the oxidizing power can be enhanced by adding potassium nitrate (KNO_3) or sodium nitrate ($NaNO_3$). Lithium borates or acid digestion largely replaced Na_2CO_3 and NaOH fluxes because of impurities in and undesirable physical properties of the Na_2CO_3 and NaOH fluxes (for example, NaOH is highly hygroscopic and froths and spurts on heating).
Lithium metaborate ($LiBO_2$) and tetraborate ($Li_2B_4O_7$)		x	No	$LiBO_2$ and $Li_2B_4O_7$ are non-oxidizing fluxes that have been used to decompose geologic samples. $Li_2B_4O_7$ is more acidic (has a higher boron trioxide (B_2O_3) content) than $LiBO_2$; consequently, $LiBO_2$ is a better flux for acidic rocks (high silica) and $Li_2B_4O_7$ is better for basic rocks (low silica). Zircon, some metal oxides, some rare earth phosphates, the rare earth fluoride, fluorcerite, and many sulfides are only partially decomposed, and additional treatment before or after fusion is necessary for samples containing these minerals. Roasting samples prior to fusing is a common approach for samples with considerable sulfide minerals.
Sodium peroxide (Na_2O_3)	x		Yes	Na_2O_2 is a powerful oxidizing alkali flux. Many refractory minerals including chromite, zircon, rutile, ilmenite, bauxite, beryl, titanite, and cassiterotantalite are decomposed by heating with Na_2O_2. Sulfides, arsenides, rare earth phosphates, W, Nb, and Ta minerals, zirconium oxides, and vanadates also are effectively decomposed. Flux-to-sample ratio normally is 5–10 or greater but can be reduced to 1–2 to reduce the salt content of the final solution. The low-flux ratio is called "sintering."

USGS